

Material science - a trip to materials and their applications

Janusz D. Fidelus

janusz.fidelus@gum.gov.pl

ROAD MAP

- Selected applications of carbon materials;
- Examples of challenges related to renewable energy;
- Oxide nanopowders doped with rare earths for technical and medical applications;
- Other application examples
- Potential directions of cooperation with GUM

ROZPRAWA DOKTORSKA

Janusz Fidelus

**"BADANIA
NAD OTRZYMYWANIEM POWŁOK
Z WĘGLA SZKŁOPODOBNEGO
NA POWIERZCHNI KOMPOZYTÓW
WĘGIEL - WĘGIEL"**

*Promotor pracy:
prof.dr hab. inż. Stanisław Błażewicz*

AGH University of Science and Technology, Cracow

Potential application:

1.

Construction elements of vacuum systems operating at elevated temperatures under mechanical load conditions (e.g. construction elements of particle accelerators)

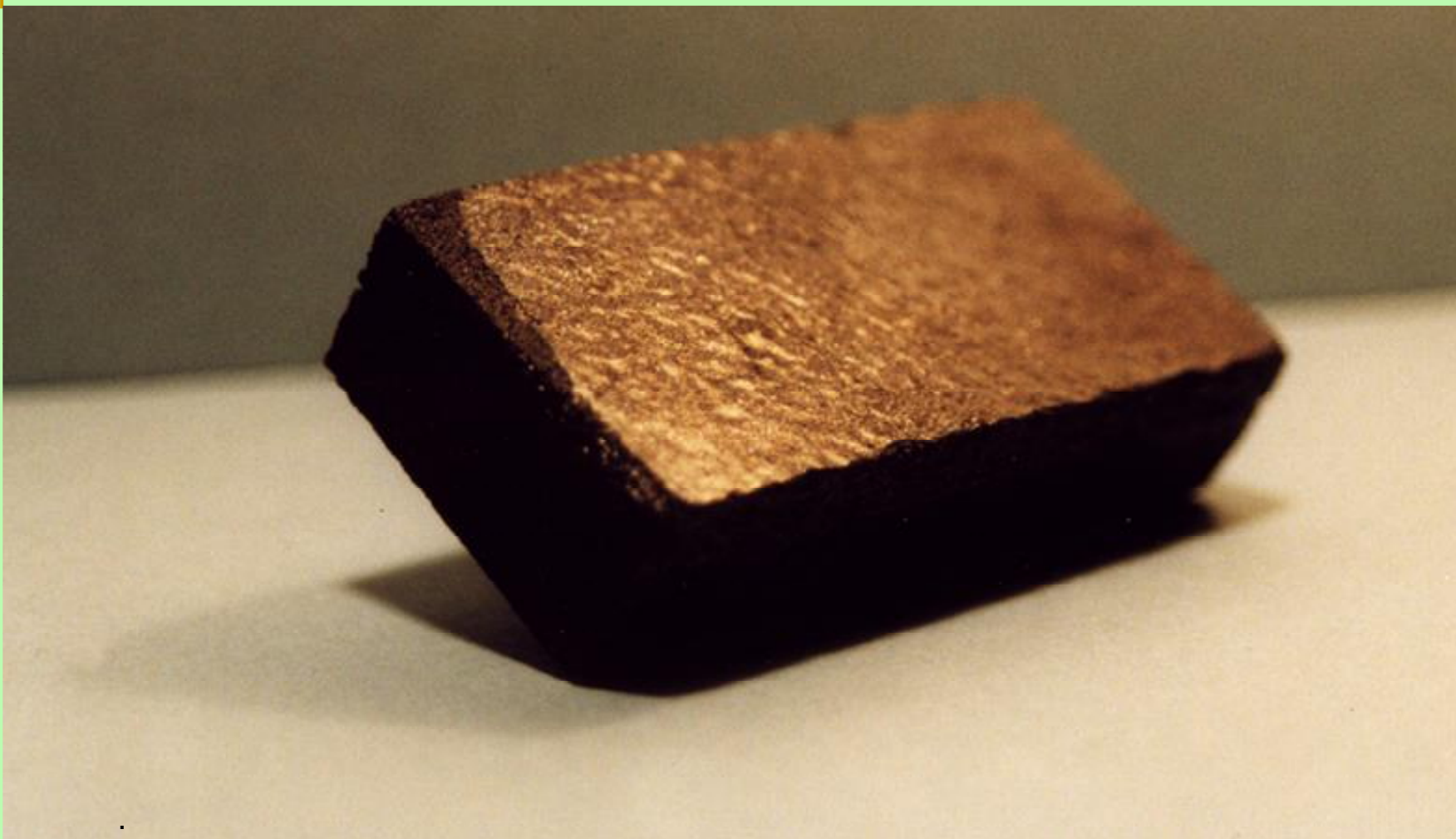
2.

Constructive elements that work in aggressive, non-oxidizing chemical environments

3.

Constructive implants in orthopedics

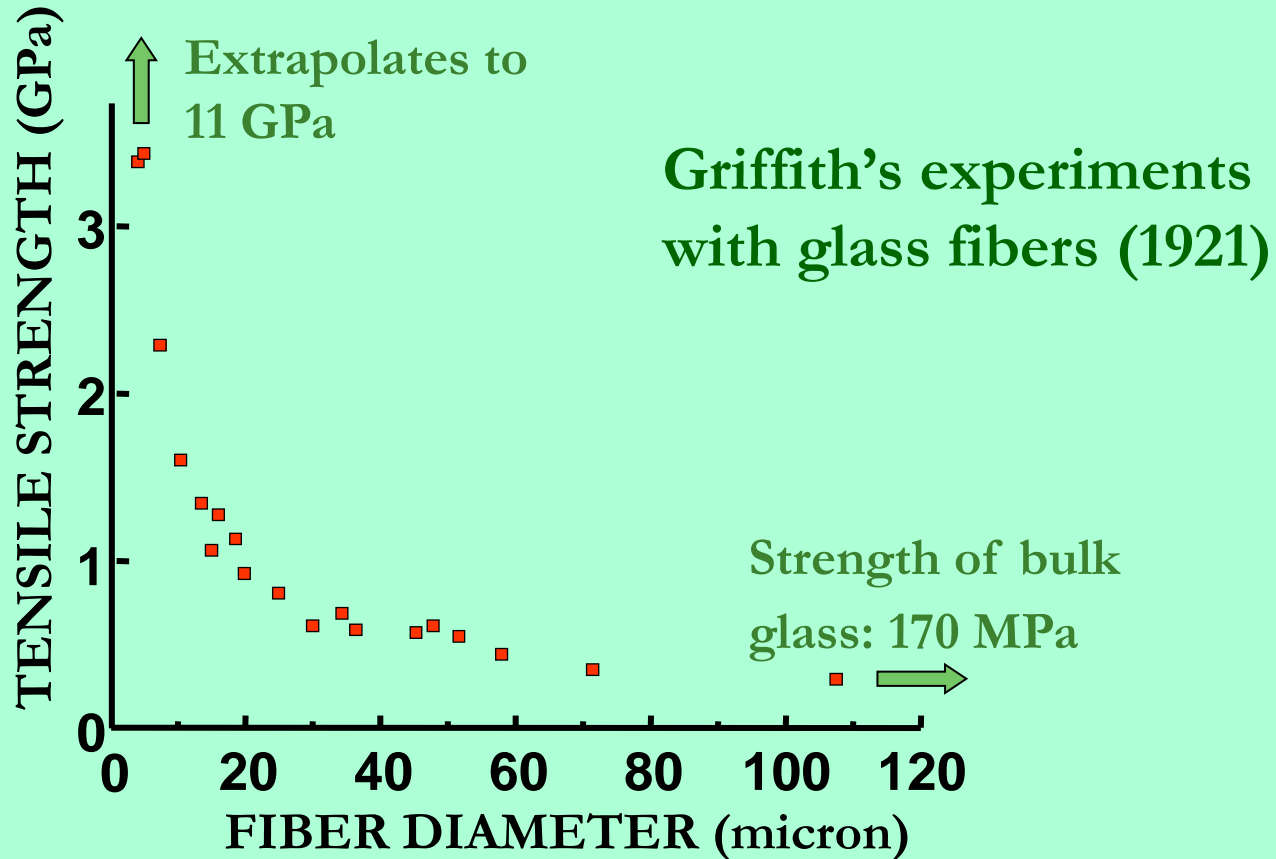
Glass-like carbon coated C/C composite



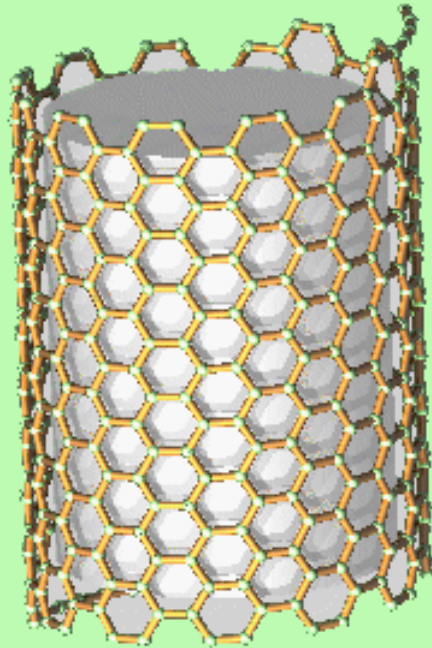
Fidelus J. et al. Patent RP nr PL – 337 136, *Sposób wytwarzania kompozytu węgla-węgiel.*

Fidelus J. et al. Patent RP nr PL- 346 251, *Sposób wytwarzania węgla szklopodobnego.*

Why decrease the size of the dispersed phase?



Carbon Nanotubes

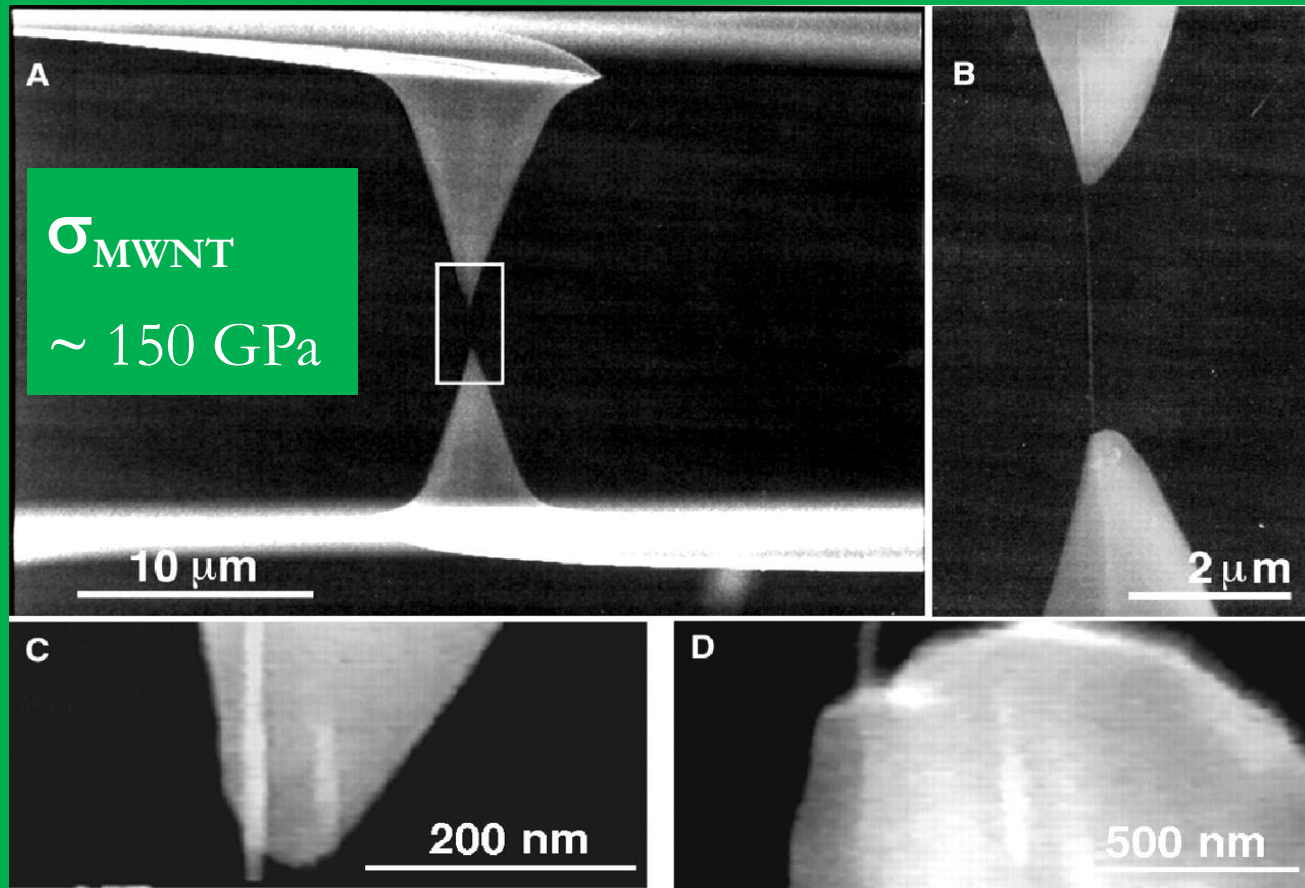


1991 – Iijima

Young's modulus of up to 1.2 TPa
Strengths of up to 20-200 GPa

Nanocomposites?

TENSILE STRENGTH OF MWNT



Min-Feng Yu et al, Science (2000)

Please note the significance of fiber aspect ratio (length/diameter) and fiber-matrix interfacial area.

Take a 10 cc composite consisting of 60% carbon fibers in a polymer. Fiber diameter = **5 micron**. Total length of fiber is $L = \text{volume}/\pi r^2$, thus $(6 \cdot 10^{-6} \text{ m}^3)/\pi(2.5 \cdot 10^{-6})^2 = \mathbf{306 \text{ km}}$. The area of fiber-matrix interface is $S = 2\pi rL = \mathbf{4.8 \text{ m}^2}$.

Now take 1% single-wall carbon nanotubes (SWNT) in the same composite volume. Tube diameter is **1 nm**, total tube length is $L = (0.1 \cdot 10^{-6} \text{ m}^3)/\pi(5 \cdot 10^{-10})^2 = \mathbf{127 \cdot 10^6 \text{ km}}$ (almost the distance to the sun...) and the interface area is **399 m²** !

*(This provides an understanding of the difference between **micro** and **nano**...)*

Traditional composites versus nanotube-based composites

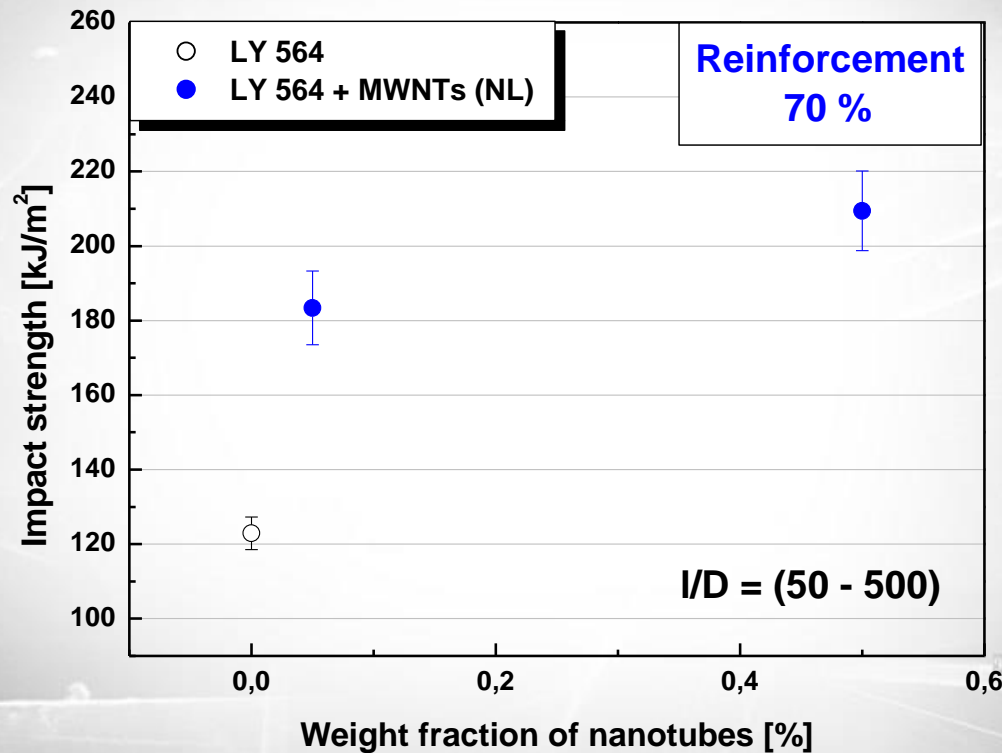
Traditional composites:

strong interface \Leftrightarrow high strength \Leftrightarrow low toughness
(and vice-versa)

Nanotube-based composites:

strong interface \Leftrightarrow high strength \Leftrightarrow high toughness!
weak interface \Leftrightarrow low strength \Leftrightarrow high toughness!

Epoxy resins and its reinforcement with low weight fraction of carbon nanotubes



J. D. Fidelus et al., Composites Part A:
Applied Science and Manufacturing (2005)

Interesting applications of carbon nanotubes

Surface probe microscope (SPM) tip: ability to manipulate a single molecule

The design of nanotube composites for tailored electromagnetic (EM) radiation shielding

The elaboration of nanotube-based synthetic muscles

The construction of space tethers and orbital structures

The 'perfect fiber' for a new generation of composites

- electron emitters
- nanotransistors
- nanocapacitors
- nano resistors
- ballistic nanowires
- sensors
- filtration membranes
- catalyst supports
- electrode materials
- gas carriers
- nanoprobes
- nanoelectronic devices
- drug deliveries
- OTHER



ROAD MAP

- Selected applications of carbon materials;
- **Examples of challenges related to renewable energy;**
- Oxide nanopowders doped with rare earths for technical and medical applications;
- Other application examples
- Potential directions of cooperation with GUM

Projects coordinated on behalf of GUM

EPM, 22RPT01 TracInd BVK-H, Traceability for indentation measurements in Brinell-Vickers-Knoop hardness.

EMPIR 19ENG05 NanoWires project „High throughput metrology for nanowire energy harvesting devices”

EMPIR 19ENG08 WinDEFY “Traceable mechanical and electrical power measurement for efficiency determination of wind turbines”

EMPIR 18SIB08 ComTraForce „Comprehensive traceability for force metrology services”



NanoWires



12 European countries and universities
17 nanotechnology laboratories

Supporting Europe's future demand for
renewable energy



NanoWires

Collaborators and Stakeholders

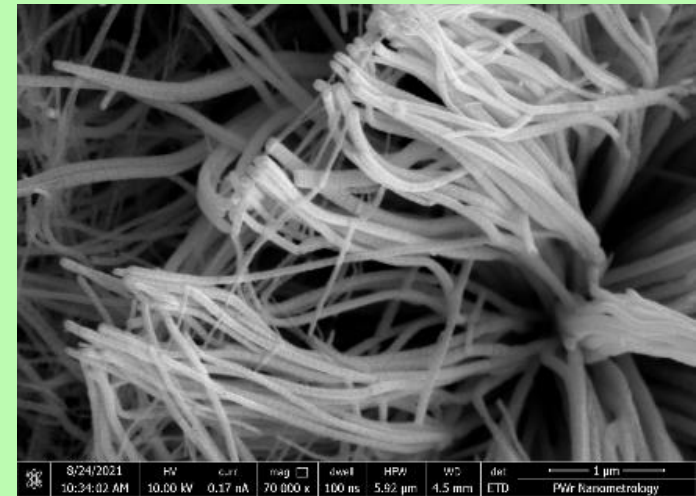
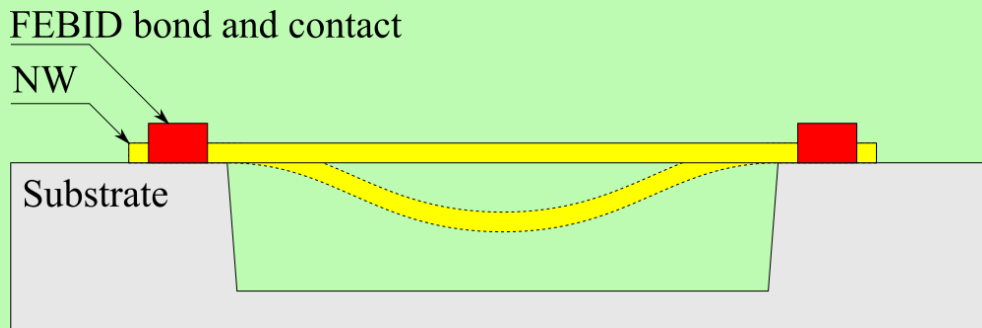
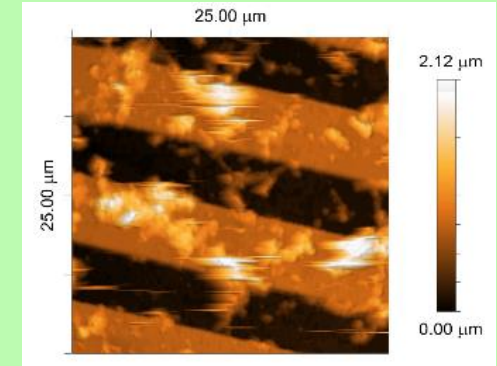


A novel method of mechanical measurement of single nanowires on specialized substrates using the AFM method

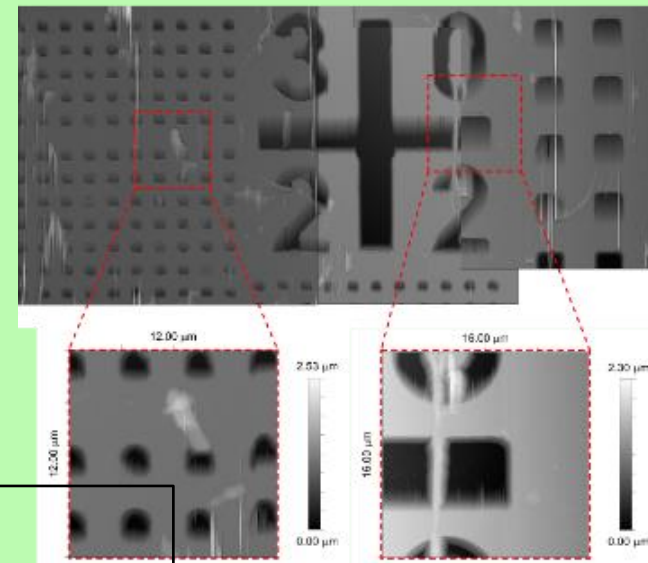
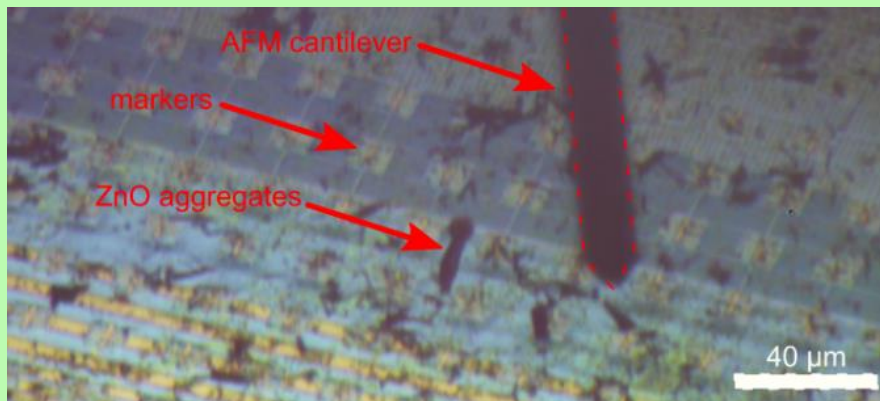
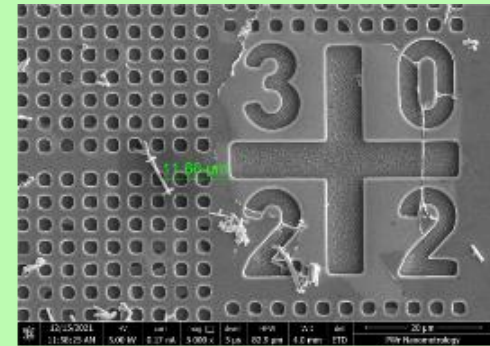
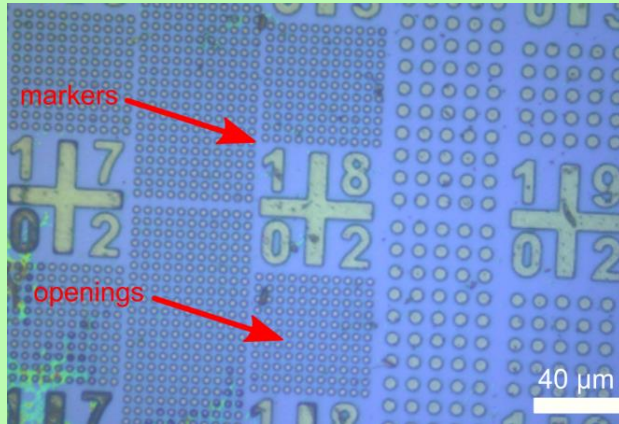
A novel method of mechanical measurement of single nanowires on specialized substrates using the AFM method

How to measure nanowire?

- Particles more or less repeatable
- Chaotic placement
- Particles have to be delivered onto substrate
- Without proper substrate – chaotic placement



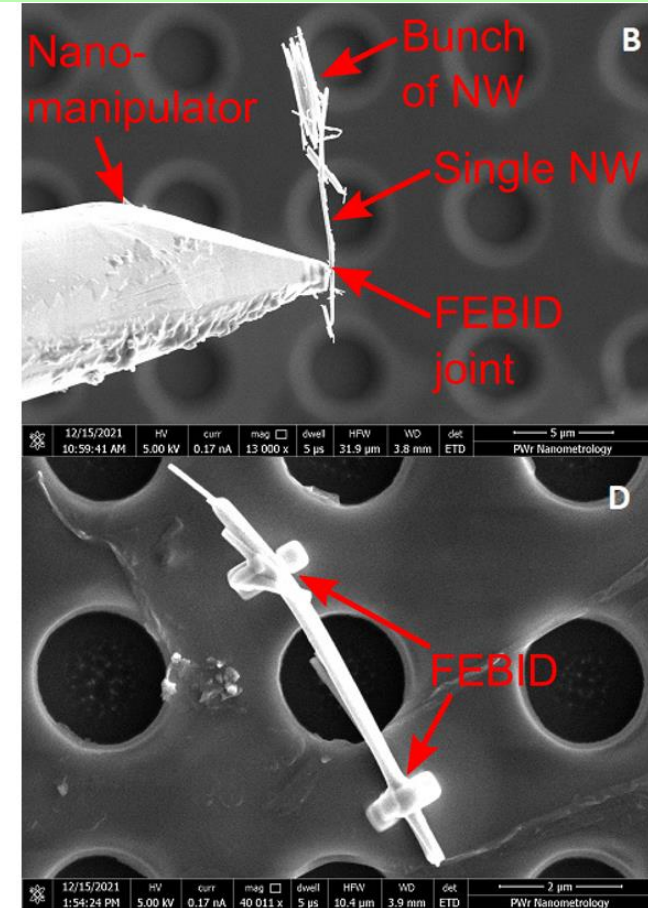
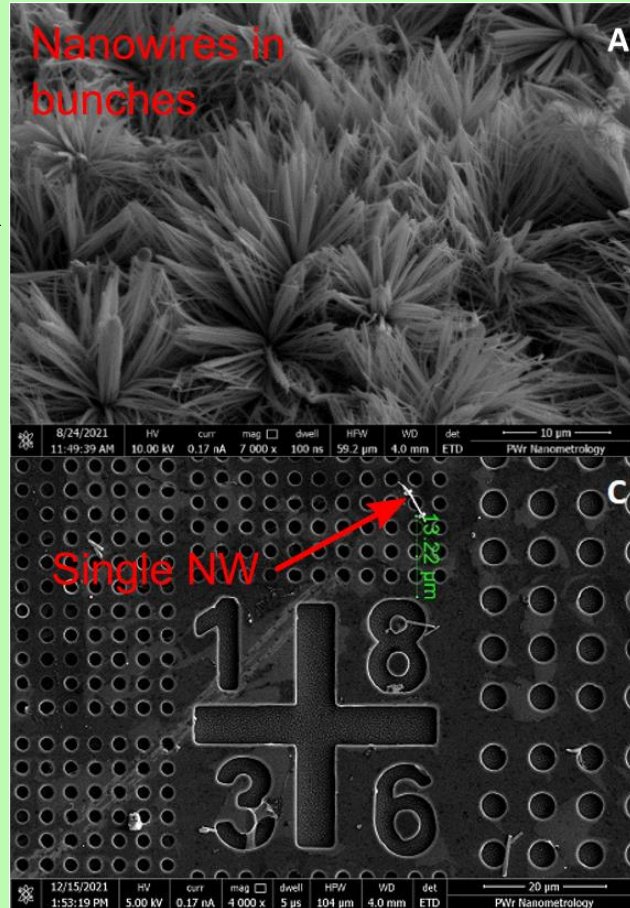
Designed metrological substrates



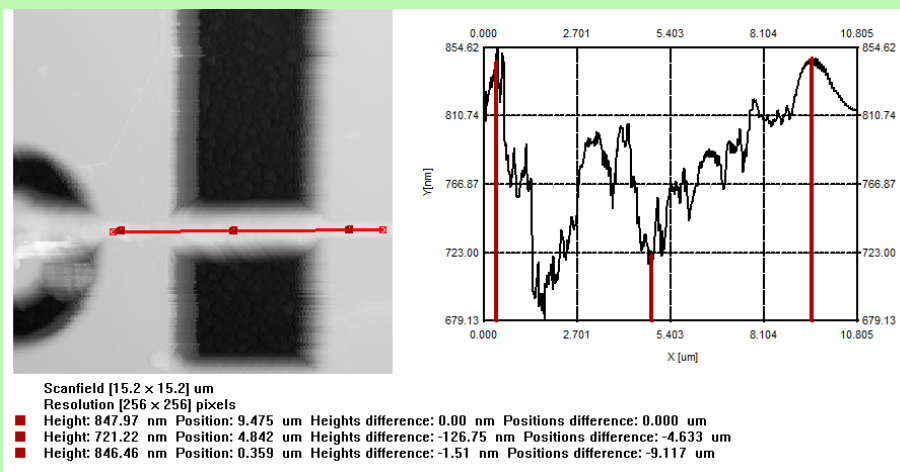
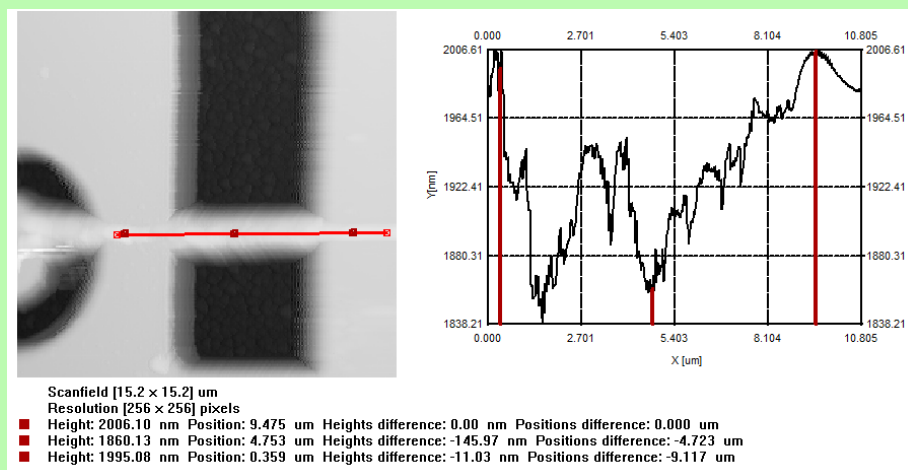
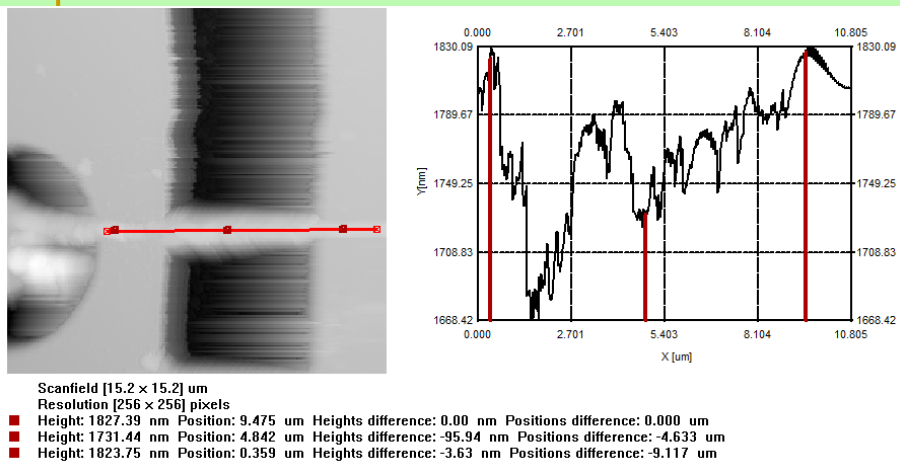
Substrates consisted of nanocrystalline $\langle 100 \rangle$ silicon wafers covered with 1 μm silicon oxide. In the oxide layer, openings were made. They were defined precisely by a photolithographic process. Processing of the oxide layer was performed with dry plasma etching.

Nanowires FEBID operations

- Transfer to the desired location
- Bonding with material deposited using a focused electron beam
- Repeatable measurements of single and same nanowire



Measurement of mechanical properties on a substrate



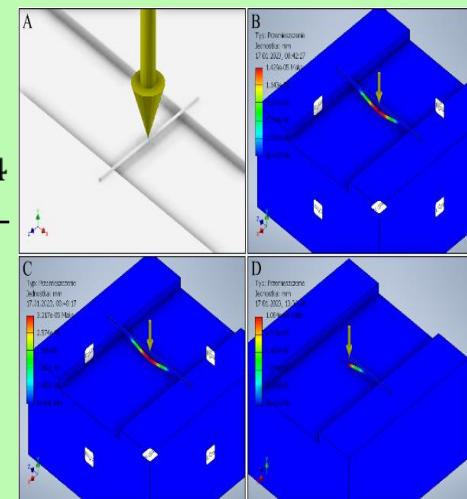
$$F = 900 \text{ nN}$$

$$l = 1,5 \text{ } \mu\text{m}$$

$$I = \frac{\pi \phi^4}{64} = \pi \cdot \frac{300^4 \text{ nm}^4}{64}$$

$$\Delta z = \frac{Fl^3}{6EI}$$

$$\Delta z = 24 \text{ nm}$$



Theoretical value of E : 100 GPa

$$E_{meas} \approx 53 \text{ GPa}$$

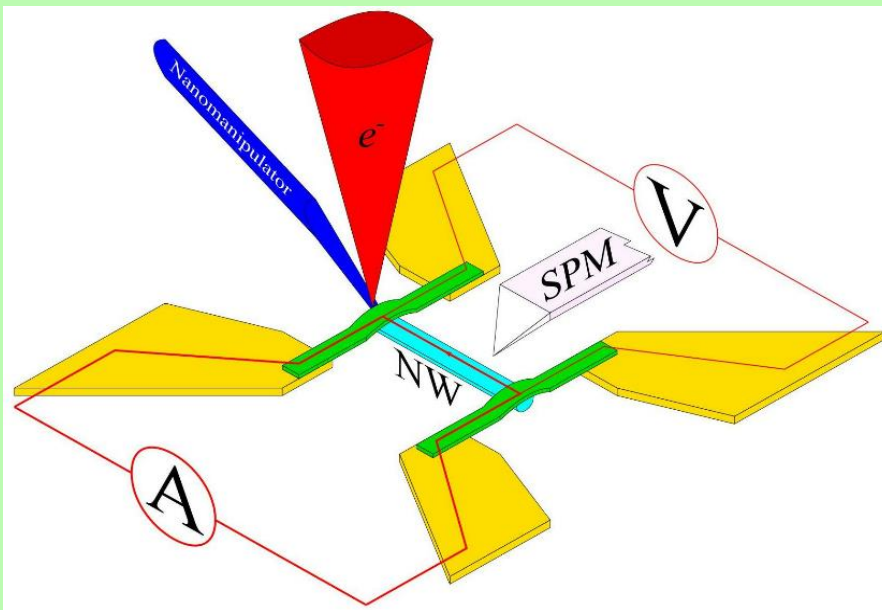


The EMPIR initiative is co-funded by the European Union's Horizon 2020 research and innovation programme and the EMPIR Participating States

A novel method of mechanical measurement of single nanowires on specialized substrates using the AFM method

The research is crucial for identifying the links between synthesis, structure, and property that, in turn, lead to the optimization of harvesting devices, biological systems, sensors, and many others.

Setup for correlative electromechanical investigations of nanowires with scanning probe microscopy



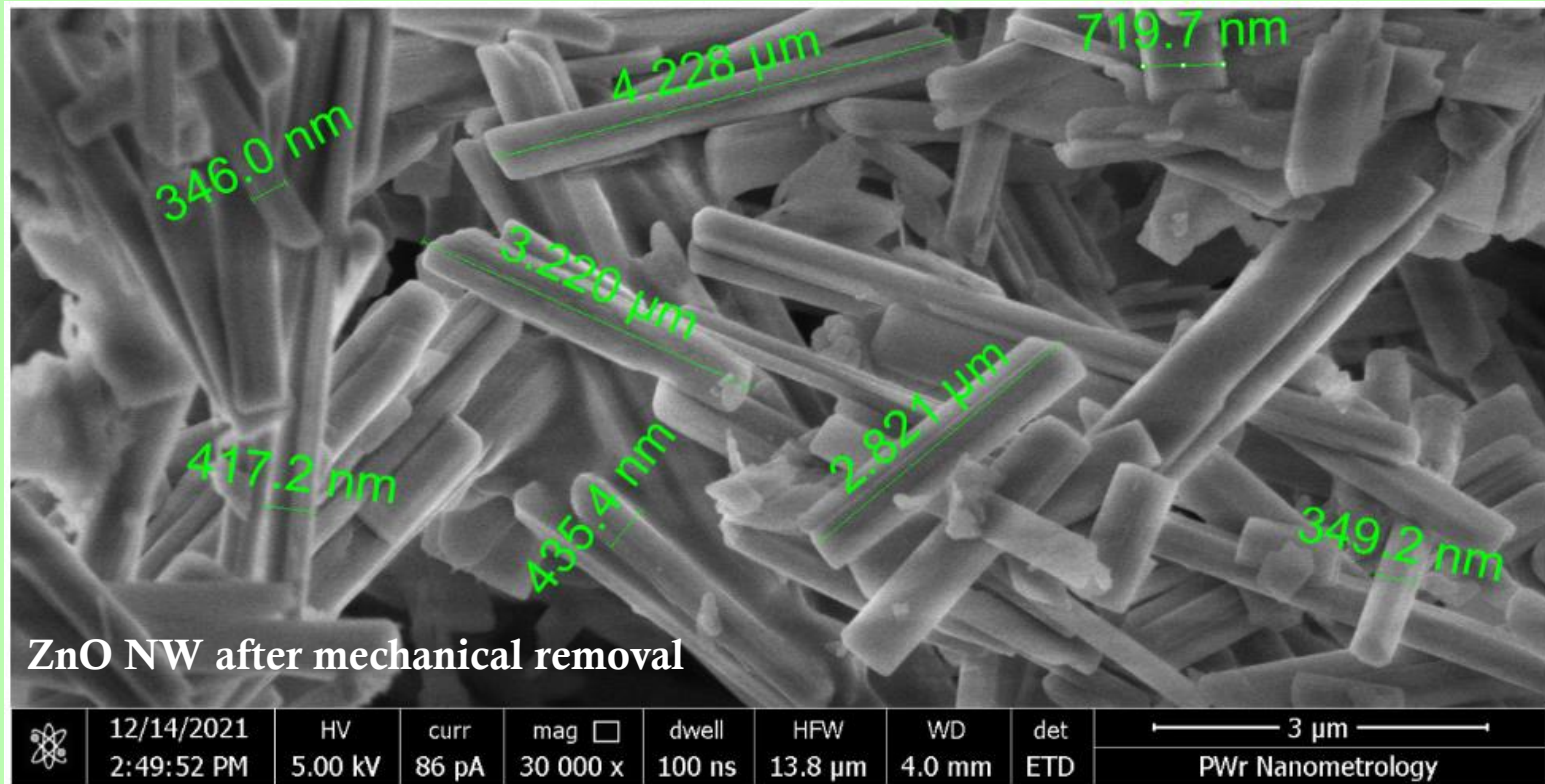
Setup schematic with all processes' stages involved – nanomanipulation, FEBID deposition, electrical measurement and SPM.

Nanomaterials **2023**, 13(17), 2451

Setup for correlative electromechanical investigations of nanowires with scanning probe microscopy

Nanowires

Investigated were zinc oxide (ZnO) nanowires with length of about 2 μm and mean diameter 120 nm for single NW. They were obtained by anodic oxidation of Zn foil in a 10 mM sodium bicarbonate electrolyte and thermal post-treatment. They were removed mechanically and transferred onto the Si substrate.

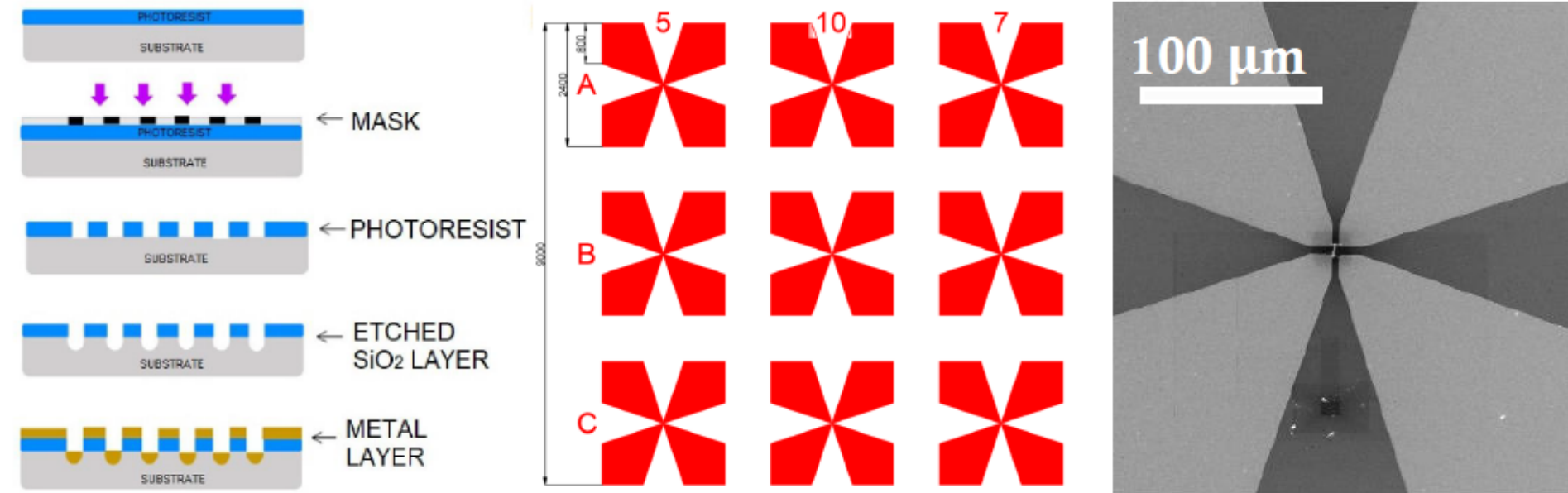


Nanomaterials **2023**, 13(17), 2451

Setup for correlative electromechanical investigations of nanowires with scanning probe microscopy

The substrate

Substrates were gold patterned over silicon oxide (SiO_2) in order to create smooth milli-to-micro meter contacts for connecting the NW with macroscopic electrical setup. Single chip consisted of nine separate devices; each device consisted of four metal contacts. Gold and oxide were at even level for no mechanical pre-tensioning.

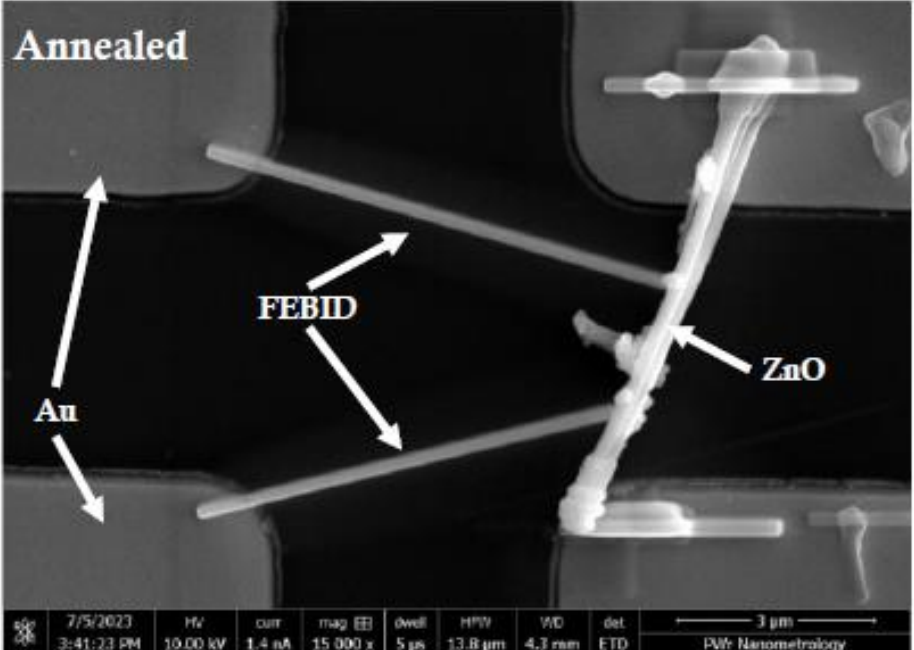
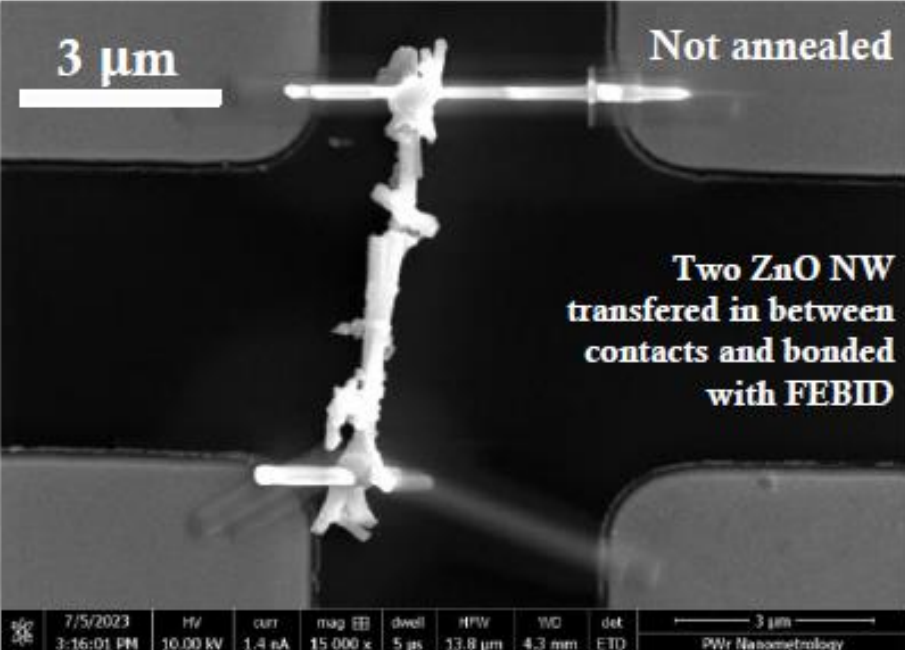


Substrates in: cross-section with fabrication steps shown, chip layout and single device SEM image.

Setup for correlative electromechanical investigations of nanowires with scanning probe microscopy

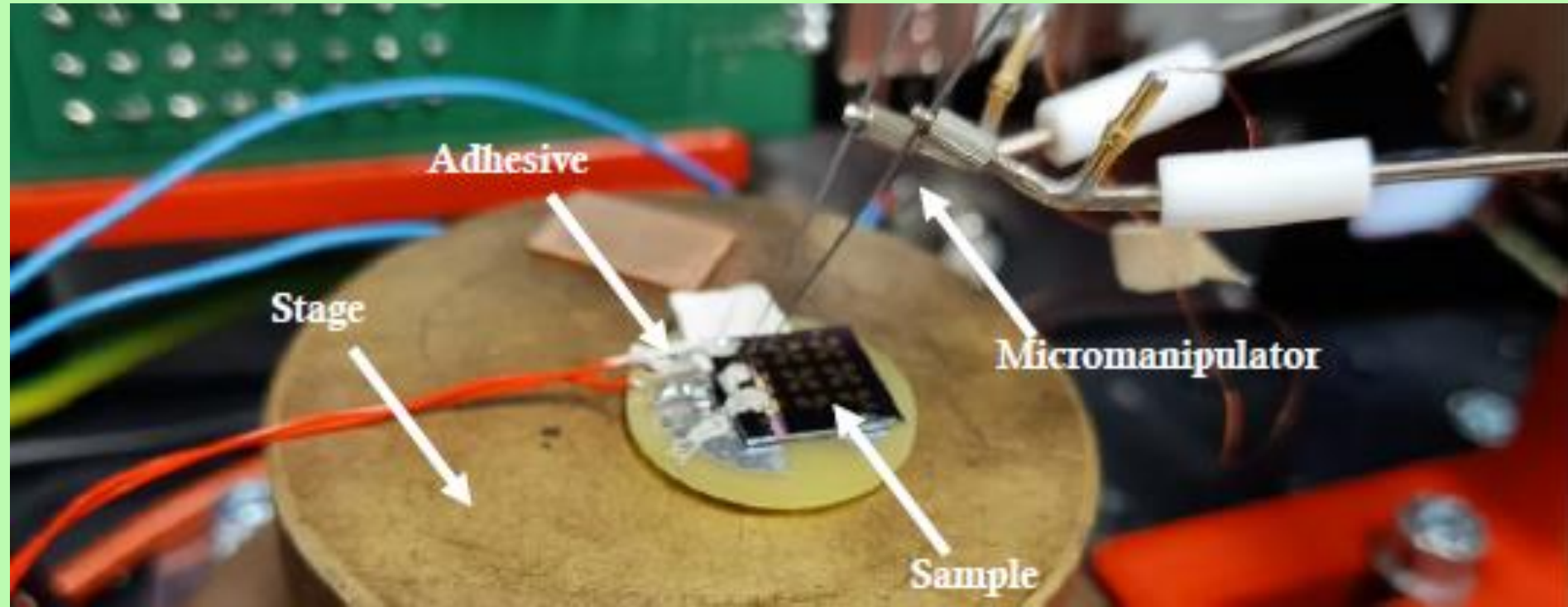
Measurement

NWs were carried with Easy Lift nanomanipulator in FEI Helios NanoLab 600i Dual Beam microscope chamber. Only adhesive force was used, introducing no chemical modification. They were then bonded with surface-born focused electron beam induced deposition (FEBID). Two distinct NWs were chosen – not annealed and annealed – for comparison of resistivity.



Nanomaterials **2023**, 13(17), 2451

Setup for correlative electromechanical investigations of nanowires with scanning probe microscopy



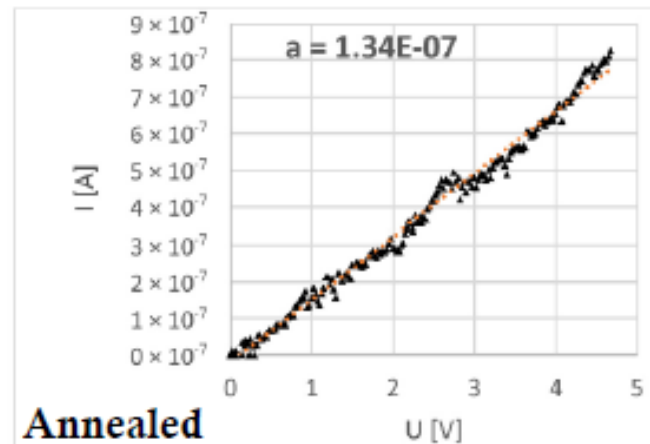
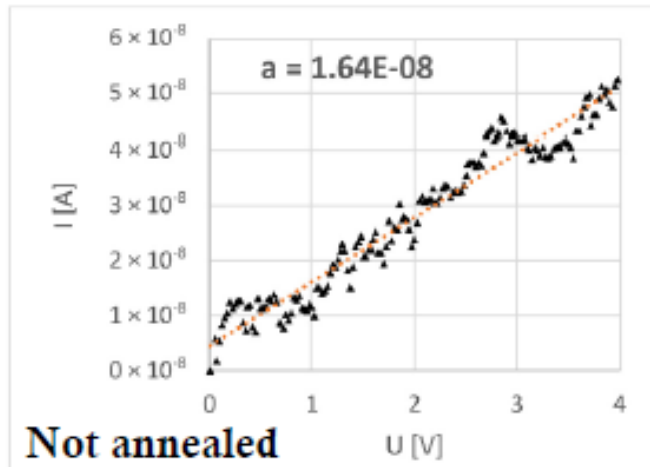
Nanomaterials **2023**, 13(17), 2451

Samples were contacted with micromanipulators and adhesive (conductive) in four-point resistance measurement setup.

Further, sample was transferred under scanning probe microscope for correlative measurement of topography and resistance.

Setup for correlative electromechanical investigations of nanowires with scanning probe microscopy

Results and outlook



I/V characteristics were measured with source measure unit Keithley 2634b. Results show order of magnitude difference in resistance and, further, resistivity.

Setup will allow for measurement of nanostructures with macroscopic devices, but simultaneously with SPM methods.

Nanomaterials **2023**, 13(17), 2451

Setup for correlative electromechanical investigations of nanowires with scanning probe microscopy

Research on the electrical properties of ZnO nanowires and related devices, described by this method, will be a useful guide not only in the design, manufacturing, and optimization of electromechanical nanodevices based on ZnO nanomaterials, but also help ensure their safe operation in future electronic applications.

Nanomaterials **2023**, 13(17), 2451

ROAD MAP

- Selected applications of carbon materials;
- Examples of challenges related to renewable energy;
- **Oxide nanopowders doped with rare earths for technical and medical applications;**
- Other application examples
- Potential directions of cooperation with GUM

Oxide nanopowders preparation using co-precipitation technique followed by microwave-driven hydrothermal process

- Preparing suitable solution
- Heating in the microwave reactor:
 $T = (250 - 330) \text{ }^{\circ}\text{C}$
 $p = (40 - 60) \text{ at}$

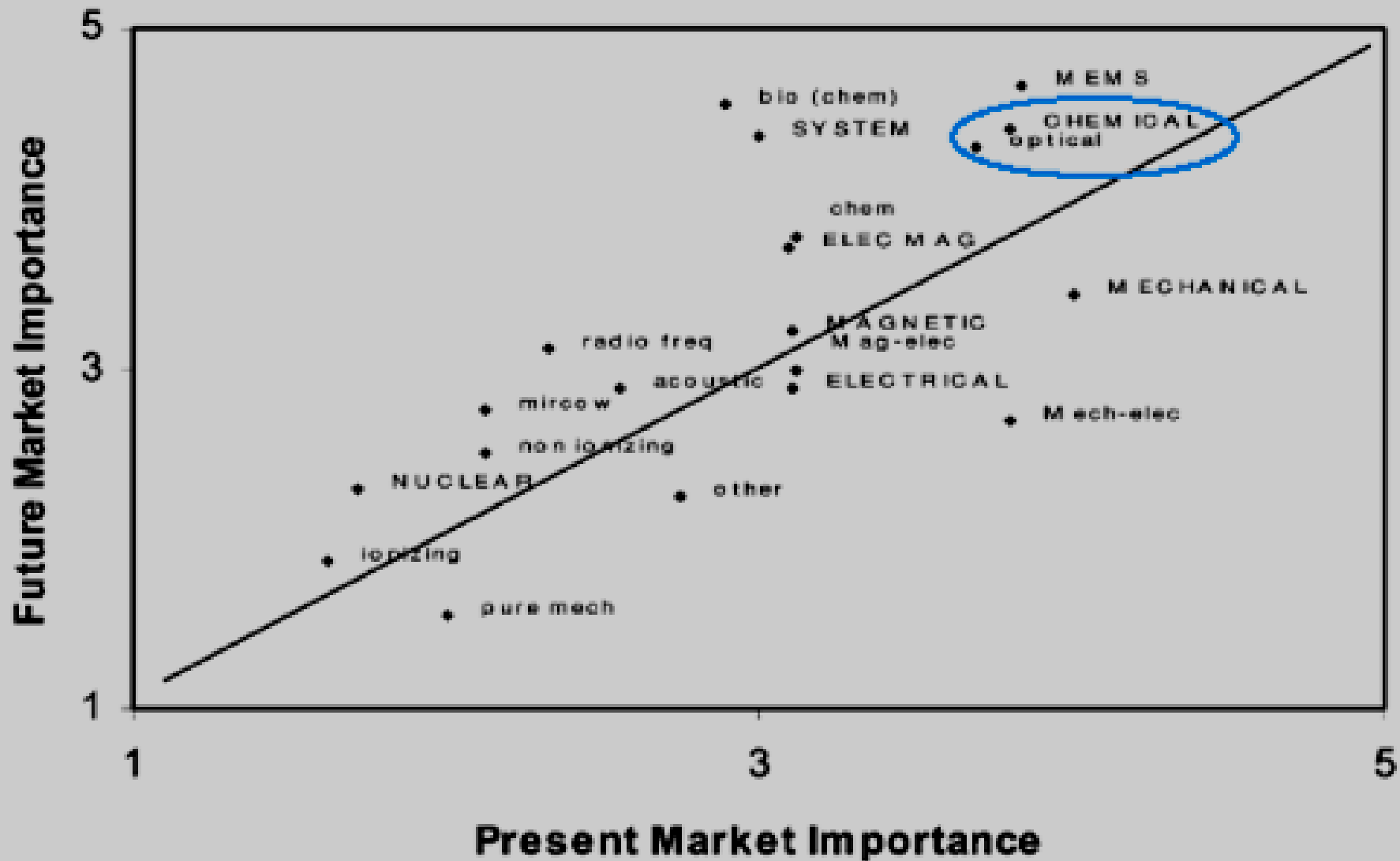
Advantages:

- High purity (Teflon vessel)
- Fast and uniform heating throughout the volume, resulting in uniform particle growth
- weak agglomerates
- possibility of functionalization during synthesis

Microwave reactor and teflon vessel



Sensor categories



ZrO₂ oxygen sensor

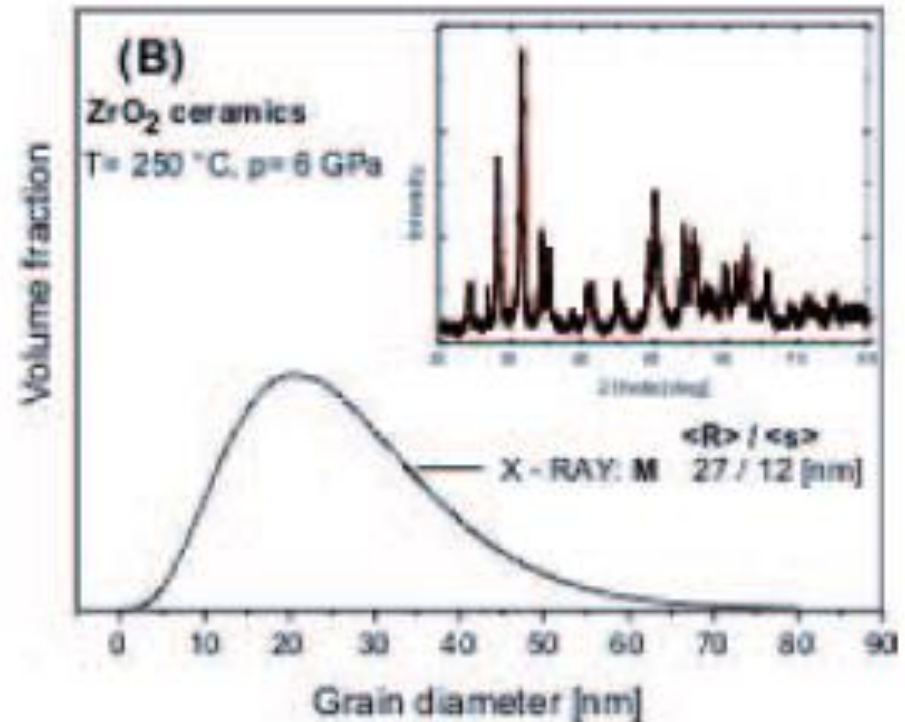
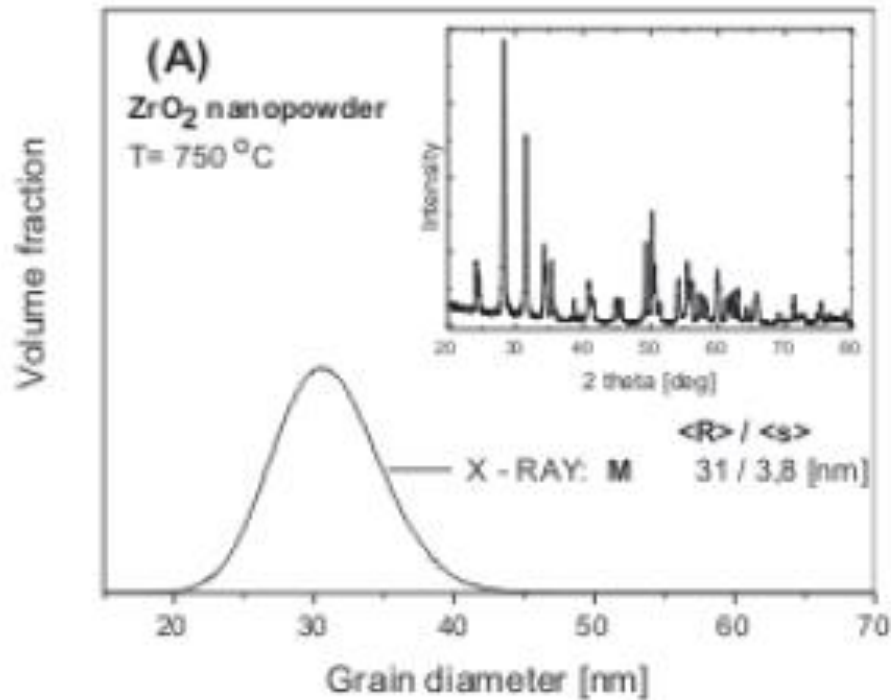


Figure. 1. GSD of the ZrO₂ nanopowder (A) and ZrO₂ nanostructured ceramics (B) obtained from analysis of the XRD data., $\langle R \rangle$ stands for average grain size, $\langle \sigma \rangle$ – for dispersion of size. The peak at 26.7 is due to sample container used during sintering. The insets document the presence of only monoclinic phase in both samples.

J.D. Fidelus et al. IEEE, art. no. 5398385, (2009)

ZrO₂ oxygen sensor

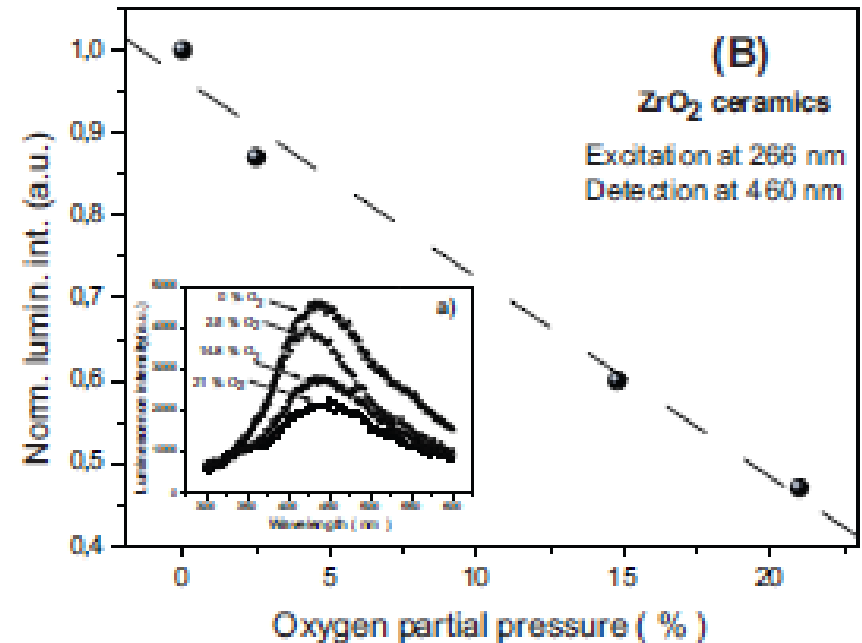
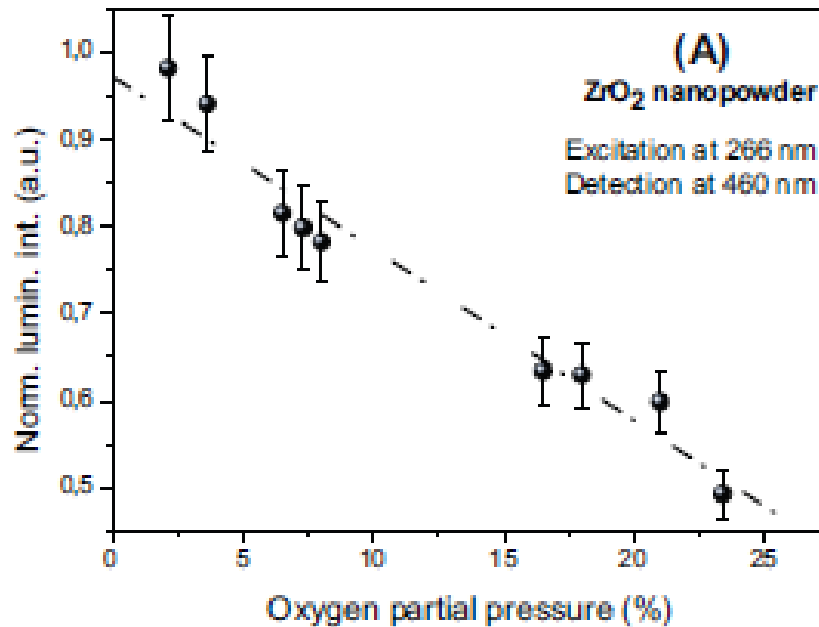


Figure 3. Luminescence intensity as a function of oxygen partial pressure for ZrO₂ nanopowders (A) and ZrO₂ nanoceramics (B) annealed in oxygen / nitrogen mixtures at 340 °C. Luminescence was measured at RT under pulsed laser irradiation. The inset a) at (B) illustrates the example of luminescence spectra for ceramics.

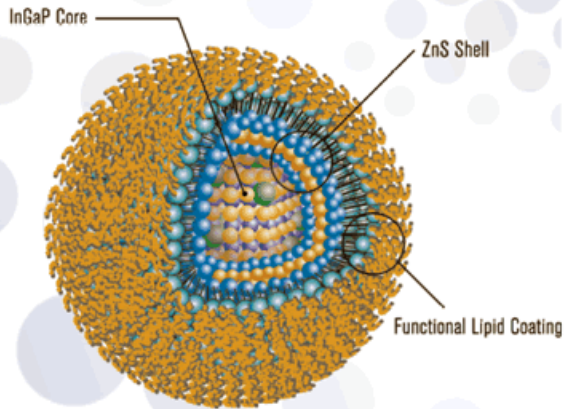
Light-converting phosphors based on yttria-stabilized zirconia

P- 387 855 – „Luminofor nieorganiczny zawierający tlenek cyrkonu oraz sposób otrzymywania tlenku cyrkonu o własnościach luminescencyjnych

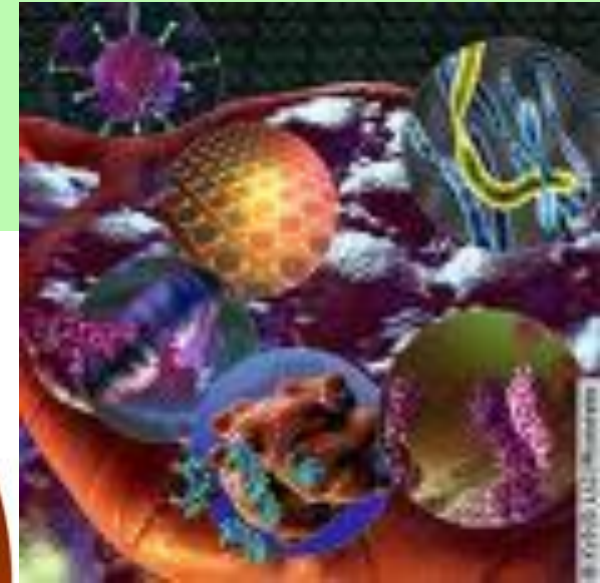
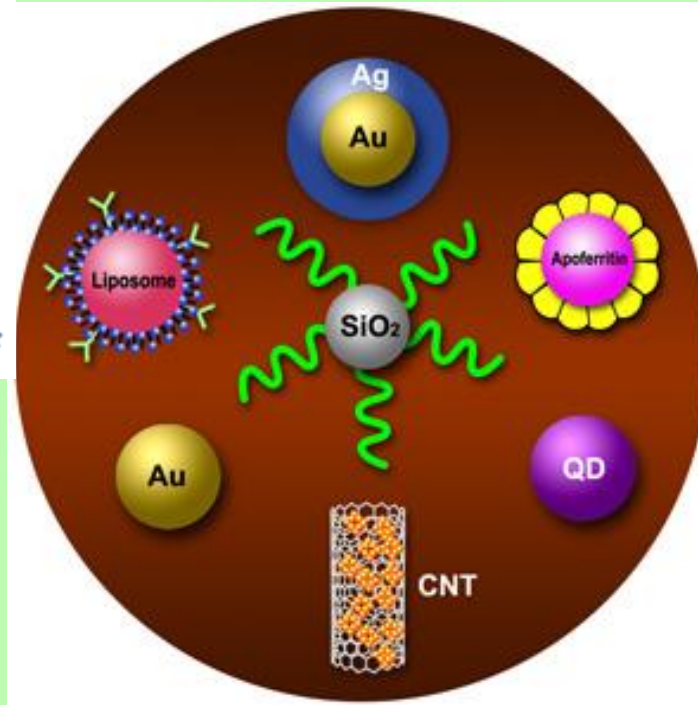
BIOSENSORS AND BIOMARKERS

T2-MP EVITAGS

Non-heavy Metal - InP Based, Water Stabilized Quantum Dots



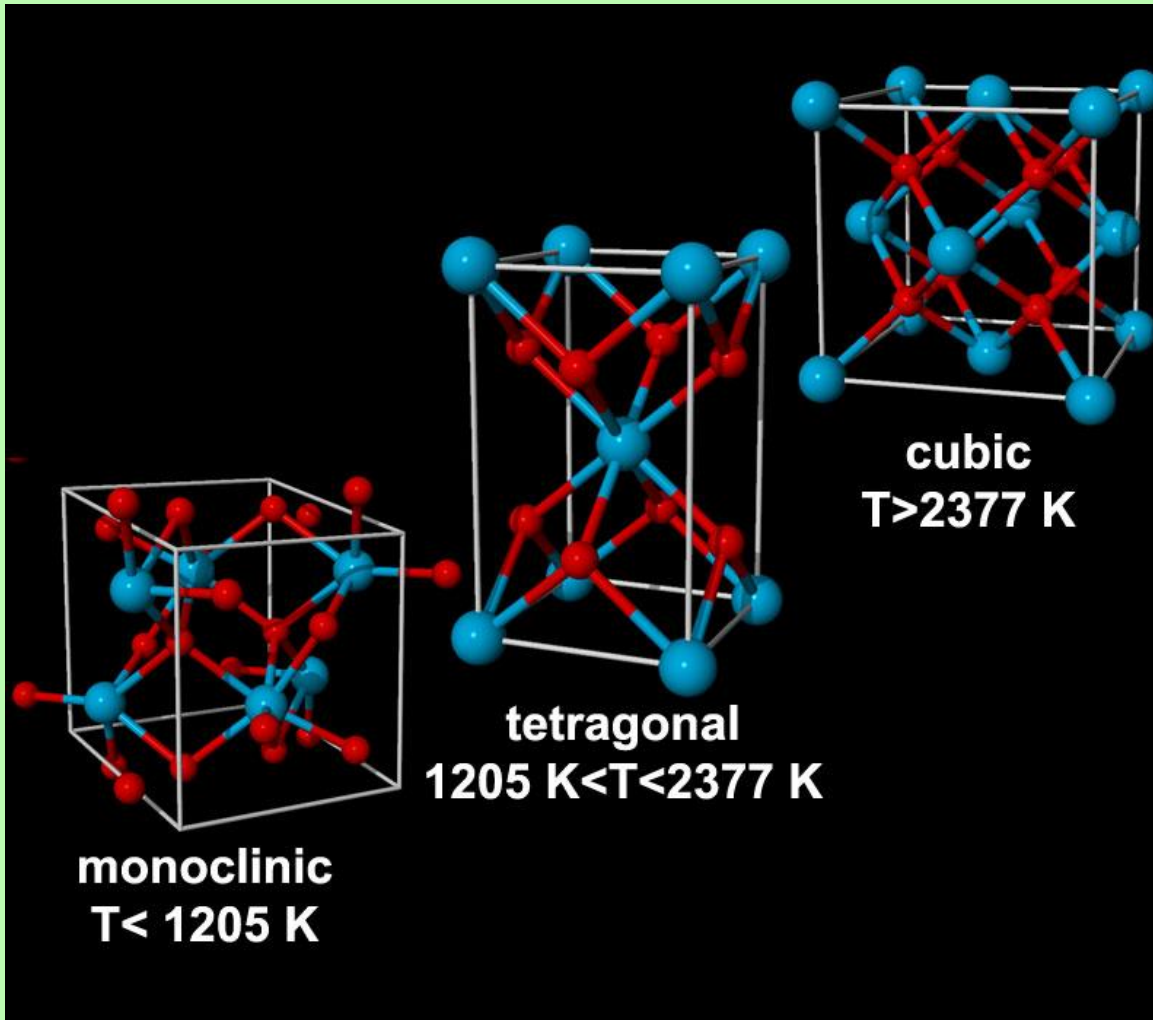
T2 - MP EviTag - InGaP/ZnS with Lipid



www.azonano.com/news.asp?newsID=960

www.pnl.gov/news/release.asp?id=273

Why phosphors based on yttria-stabilized zirconia?



Basic polymorphs of zirconium oxide

ZrO₂ – tetragonal and cubic phases



STABILIZATION

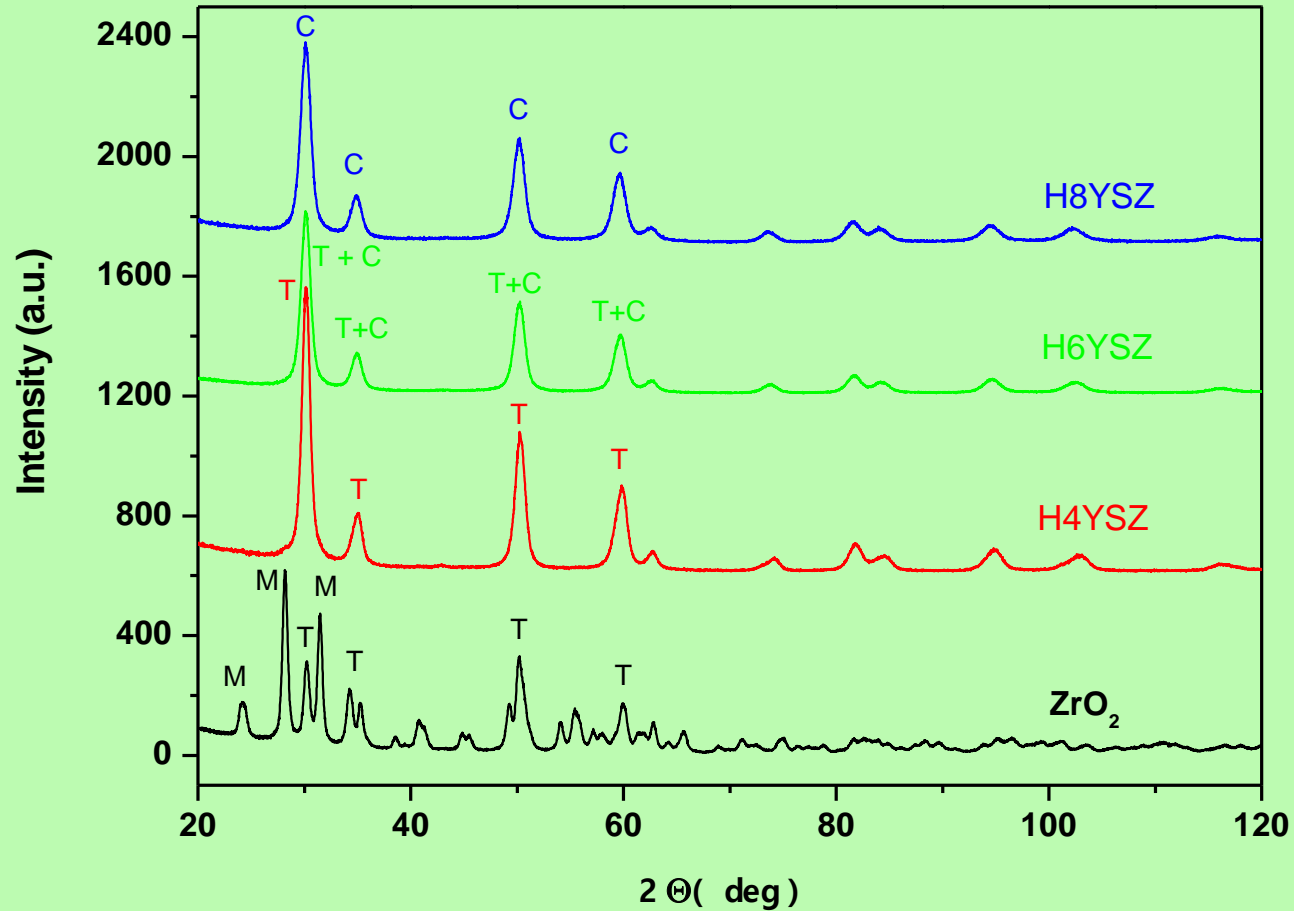
Magnesium
oxide (MgO)

Yttrium
oxide (Y₂O₃)
YSZ

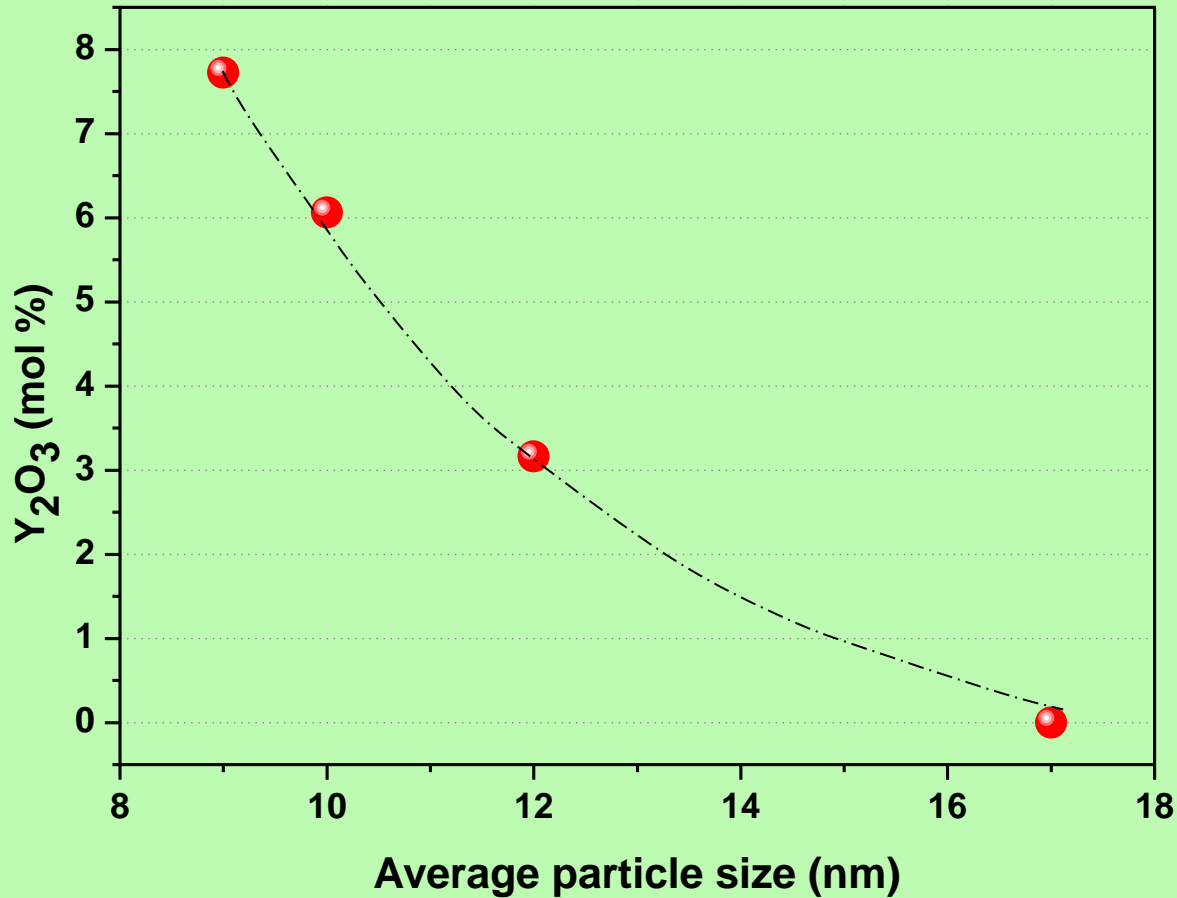
Other oxides,
i.e. Gd₂O₃

Cerium
oxide (III)
(Ce₂O₃)

Calcium
oxide
(CaO)



XRD patterns of samples Y-doped ZrO₂ after annealing at 640°C.
(M-monoclinic, T-tetragonal, C-cubic)



Molar percentage of Y₂O₃ doped ZrO₂ as a function of average particle size of ZrO₂ (from Scherrer formula) after annealing at 640°C.

Application of YSZ

Jewellery (ZIRCONIA)

because of a optical properties there is used as diamond imitation





	Name	Hardness
1	Zircon (mineral, $ZrSiO_4$)	6.5 – 7.5
2	Quartz (SiO_2)	7
3	Garnet (mineral)	7 – 7.5
4	Heliodor	7.5 – 8
5	Topaz ($Al_2SiO_4(OH, F)_2$)	8
6	Zirconia	8.5
7	Corundum (Al_2O_3)	9
8	Silicon carbide – (SiC)	9.5
9	Diamond (C)	10



Table. Minerals and their hardness

Applications of YSZ...

Medicine – Properties: hardness, shear strength and inertness



Dental implants



Endoprothesis of
the hips joint

Applications of YSZ...

Industry

- ❑ in jet engines to determine oxygen content in exhaust gases;
- ❑ to measure pH in high-temperature water;
- ❑ as membranes for high temperature solid oxide fuel cells
- ❑ as a component of waveguides
- ❑ laser mirrors and optical filters;
- ❑ for electrolytes or insulators in microelectronic devices

YSZ as substrate for epitaxial layers (commercially available)

- ❑ **YBCO film growth on CeO₂-buffered YSZ substrate by the full-solution method** [*S Wang et al 2005 Supercond. Sci. Technol. 18 1271-1274*]
- ❑ **Cyclic voltammetry of (La,Sr)MnO₃ electrode on YSZ substrate**
[*X. J. Chen et al, Solid State Ionics, Volume 164, Issues 1-2, October 2003, Pages 17-25*]

The main **aim of that work** was to extend applications of yttria-stabilized ZrO_2 nanomaterials through finding proper conditions at which the lanthanides doped nanopowders ($\text{Ln} = \text{Pr}^{3+}, \text{Eu}^{3+}, \text{Tb}^{3+}, \text{Tm}^{3+}$) exhibit good photoluminescence properties.

Pr³⁺ doped yttria stabilized ZrO₂ nanopowders preparation using co-precipitation technique followed by microwave-driven hydrothermal process

- Dissolving
 - zirconium (IV) oxide chloride octahydrate in water
 - Praseodymium (III) nitrate hexahydrate in water
 - Yttrium oxide in nitric acid
- and mixing
- Setting a pH of 10 with 1 M sodium hydroxide
- Heating (20 minutes at 100 % power in the microwave reactor, T=280 °C, p=58 at)
- Wet separation, washing with water and isopropanol
- Drying 70 °C/24h
- Grinding

Compounds i.e.:

- ZrOCl*8H₂O
- Pr(NO₃)₃*6H₂O
- 1M NaOH



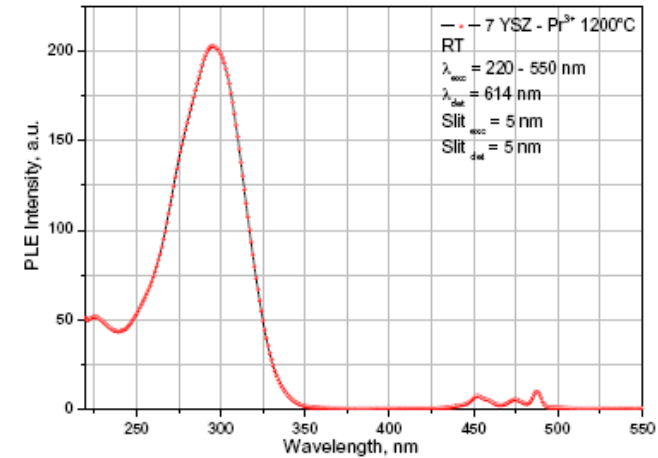
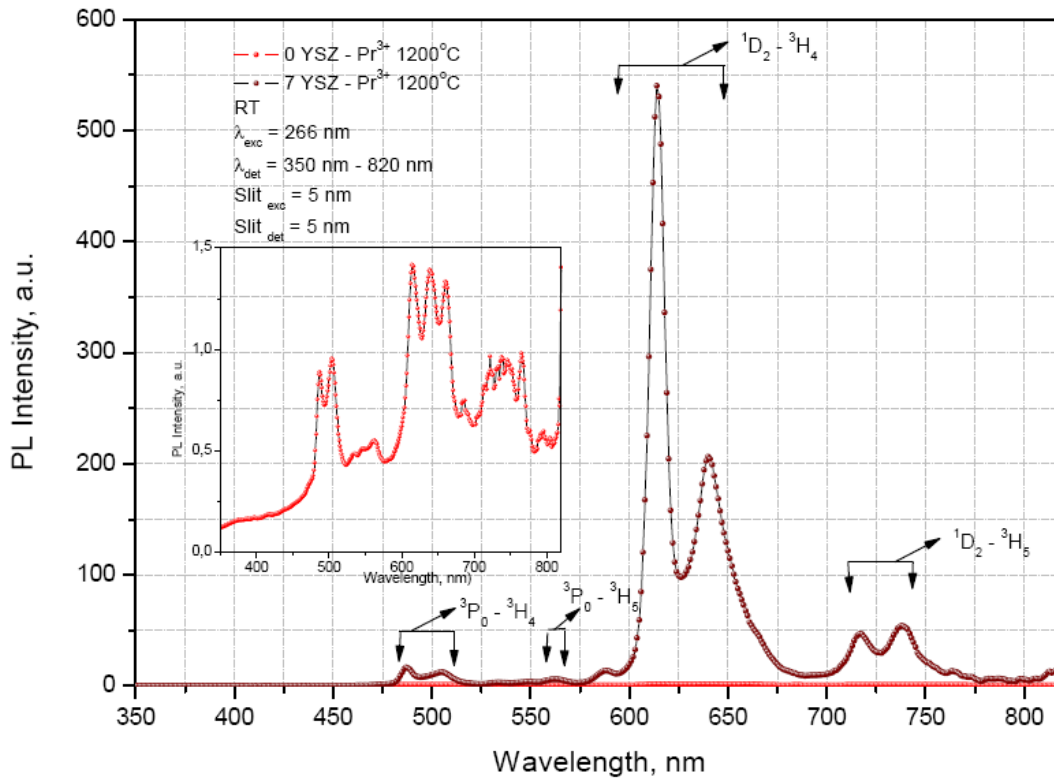


Figure 4. Photoluminescence excitation of Pr^{3+} 4f-4f emission in ZrO_2 nanopowder stabilized by 7 mol.% Y_2O_3 .

Huge intensity of PL is observed !
 PL of Pr observed in 7YSZ-0.5 Pr sample is amplified as much as 380 times.
Note that Hg vapors emit at 254 nm.

J. D. Fidelus et al. / Scripta Materialia 61 (2009) 415–418

Sample F (7YSZ-0.5Pr), 1200°C

Results of Rietveld analysis

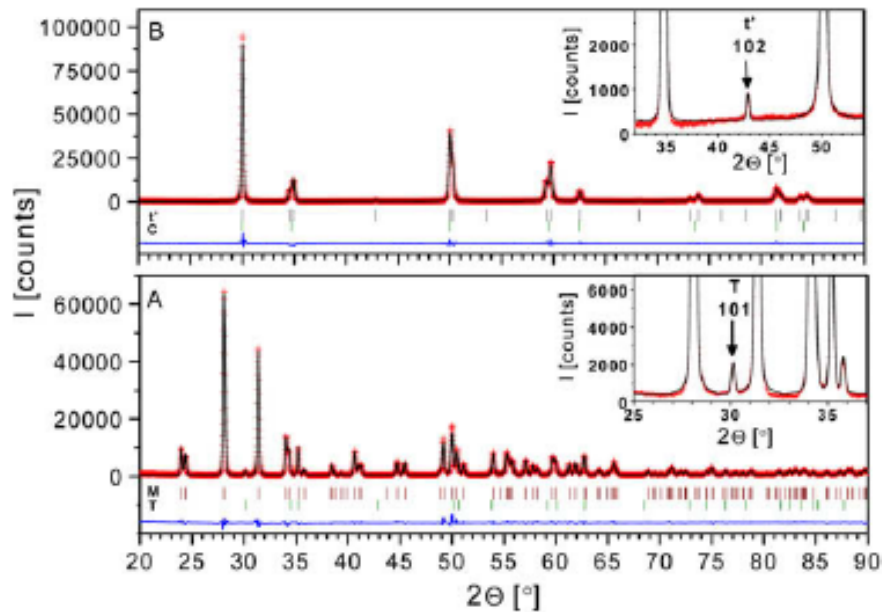


Figure 1. Results of Rietveld analysis of XRD patterns for annealed (1200 °C) nanopowders of: yttria-free sample $\text{ZrO}_2\text{-}0.5\text{Pr}^{3+}$ (A) and $\text{ZrO}_2\text{-}0.5\text{Pr}^{3+}$ with a nominal Y_2O_3 content of 7 mol.% (B). Experimental pattern is formed from points, and the solid line is the calculated profile; vertical bars labeled C, T, t' and M show the positions of diffraction peaks of the cubic, tetragonal and monoclinic phases, respectively. Difference patterns are shown below the bars. The insets document the presence of tetragonal phase in both samples. The characteristic weak reflections of this phase are indicated by arrows: 101 in (A) and 102 in (B).

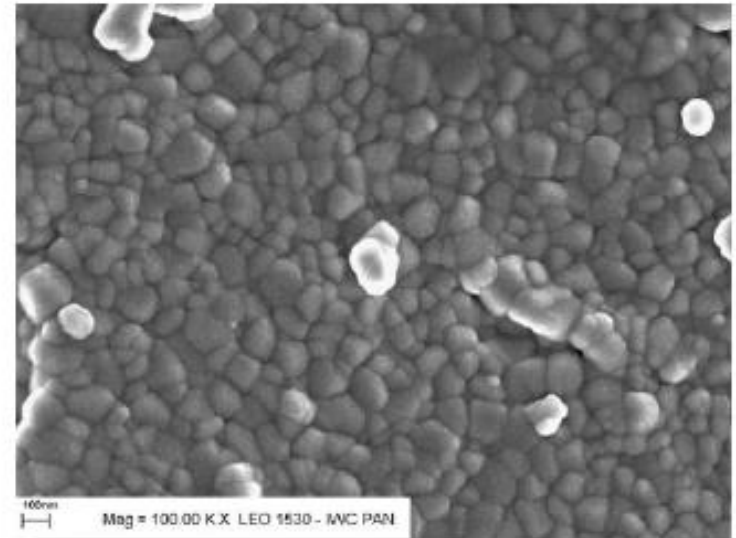
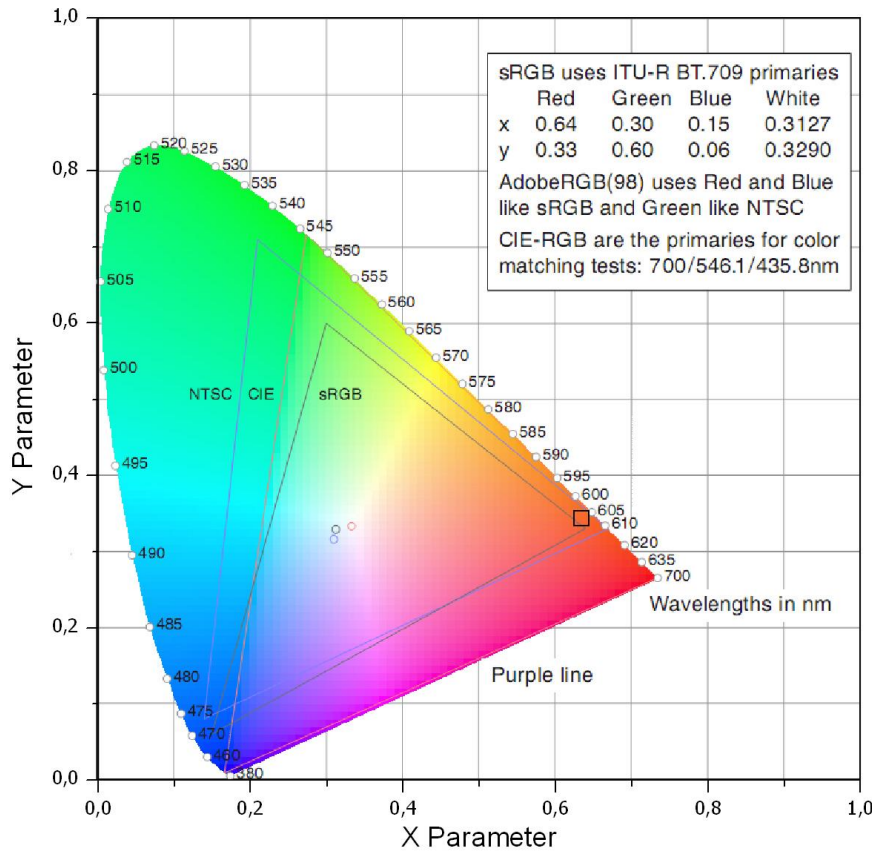


Figure 2. High-resolution SEM images of the $7\text{YSZ-}0.5\text{Pr}^{3+}$ powder after annealing at 1200 °C.

Only high-symmetry phases are present: It is a mixture of tetragonal (82 wt.%) and cubic (18 wt.%).

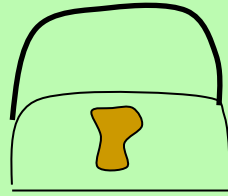
J. D. Fidelus et al. / Scripta Materialia 61 (2009) 415–418



Chromaticity diagram was calculated based on International Commission on Illumination (CIE) 1931 color space and three basic matching color functions.

For Y stabilization (7YSZ0.5Pr sample), dominant red emission of Pr^{3+} is observed.

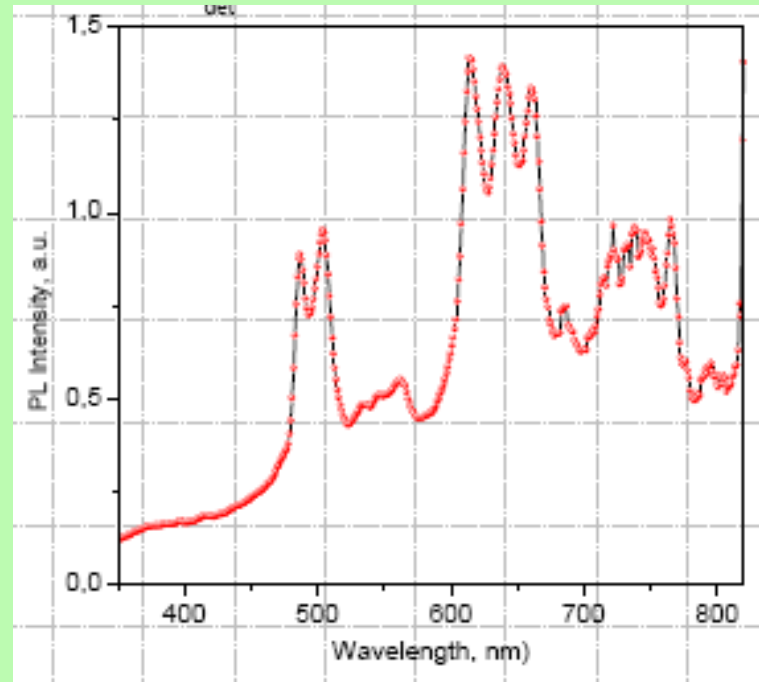
Chromaticity diagram for 7YSZ 0.5 Pr sample annealed at 1200°C



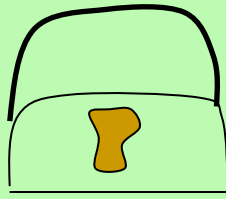
SECURITY



Papillary lines of finger



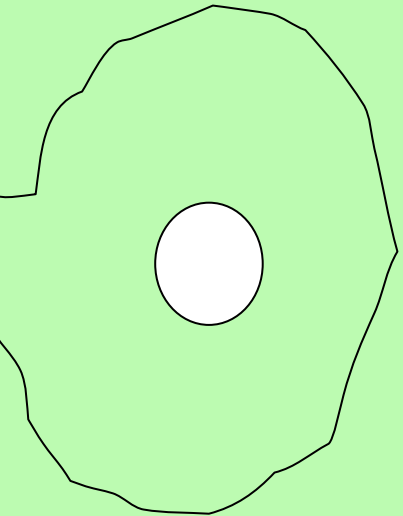
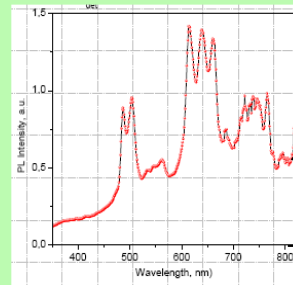
Papillary lines of optical marker



SECURITY



Papillary lines of finger



Papillary lines of optical marker

Cellulose

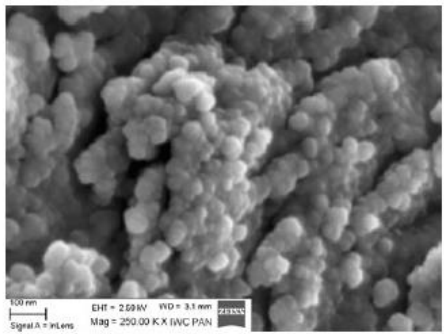


Fig. 1 High-resolution SEM photograph of 0.5 mol% of Eu^{3+} -doped ZrO_2 stabilized by 7 mol% Y_2O_3

Fig. 8 Photoluminescence spectra of pure cellulose fibers, cellulose fibers with 7YSZ-0.5Eu and reference powder by excitation at 260 nm

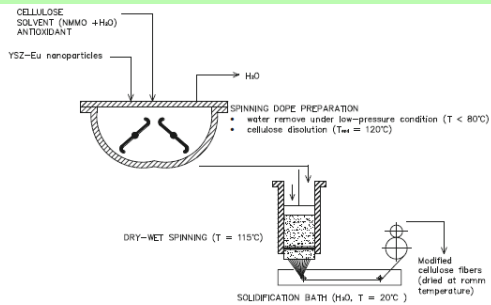
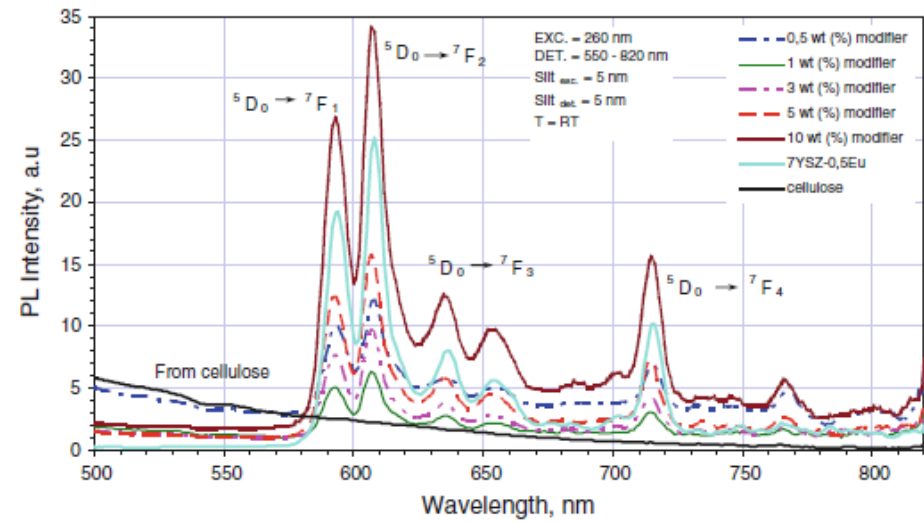


Fig. 2 Scheme and conditions for preparing modified man-made cellulose fibers in a laboratory-scale apparatus

Laboratory –scale apparatus for man-made cellulose fibers (PL)

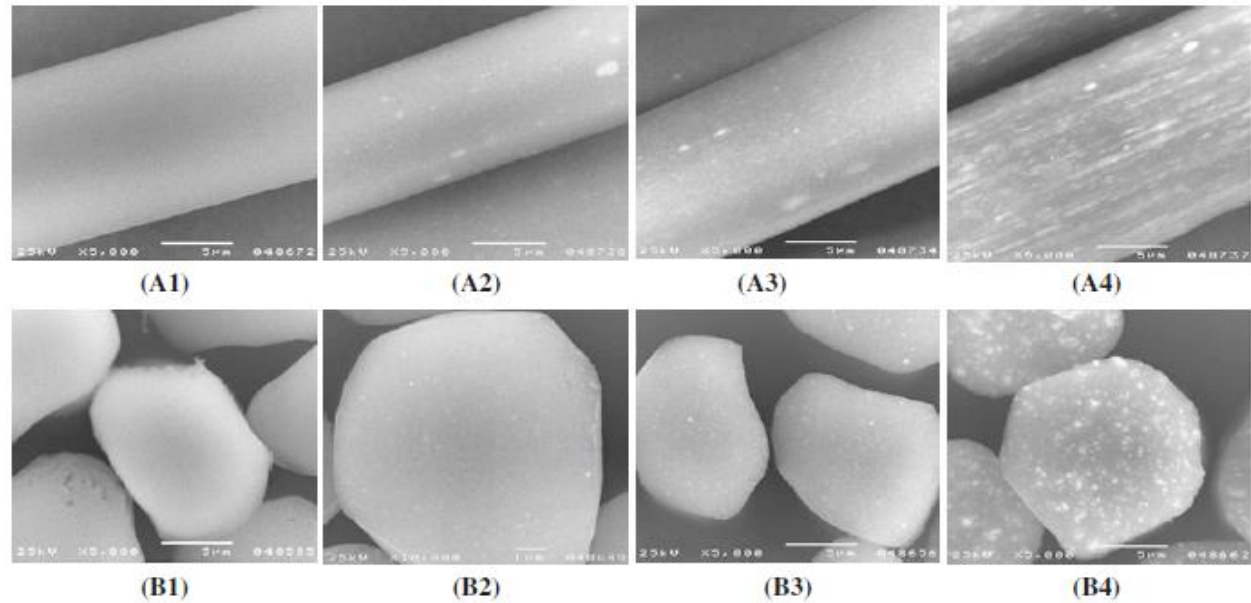


Fig. 9 SEM images of surface cellulose fibers (A1—unmodified fibers, fibers with 7YSZ-0.5Eu: A2—0.5 %, A3—5 %, A4—10 %) and cross-section (B1—unmodified fibers, fibers with 7YSZ-0.5Eu: B2—0.5 %, B3—5 %, B4—10 %)

Cellulose (2012) 19:1259–1269

ROAD MAP

- Selected applications of carbon materials;
- Examples of challenges related to renewable energy;
- Oxide nanopowders doped with rare earths for technical and medical applications;
- **Other application examples**
- Potential directions of cooperation with GUM

TiO₂:Yb³⁺ and TiO₂:Nd³⁺ -Yb³⁺ SYSTEMS

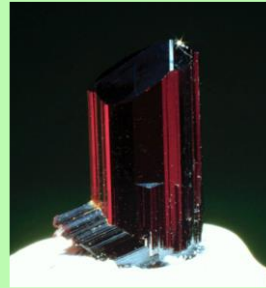
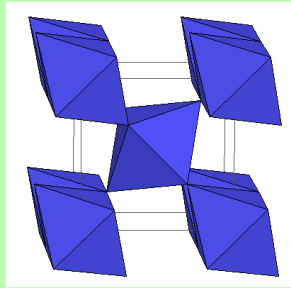


For application in solar converters or
photocatalysis and PV

Nanocrystalline titanium dioxide (TiO₂) finds wide applications in the fabrication of solar cells, fuel cells, electrical and photocatalytic systems because of it is highly stable, non-toxic and has a suitable redox potential for photodegrading pollutants.

Diagram of the mutual arrangement of the octahedrons [TiO₆] in rutile, anatase and brookite TiO₂ and the examples of naturally occurring crystals of these polymorphs

Rutile



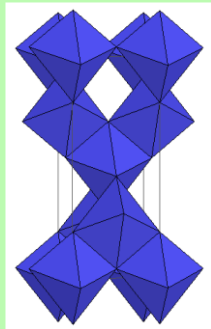
Lattice parameters of rutile:

$$a = 0,459 \text{ nm}$$

$$b = 0,459 \text{ nm}$$

$$c = 0,295 \text{ nm}$$

Anatase



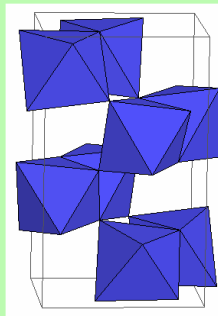
Lattice parameters of anatase:

$$a = 0,378 \text{ nm}$$

$$b = 0,378 \text{ nm}$$

$$c = 0,951 \text{ nm}$$

Brookite



Band gap for

Anatase, rutile and brookite:

$$3,23 \text{ eV}; 3,02 \text{ eV} \text{ and } 2,96 \text{ eV}$$

Ref.: J. Photochem. Photobiol. A:
Chemistry 108 (1997) 1

Optical properties of $\text{TiO}_2\text{:Yb}$ system (SPVD method)

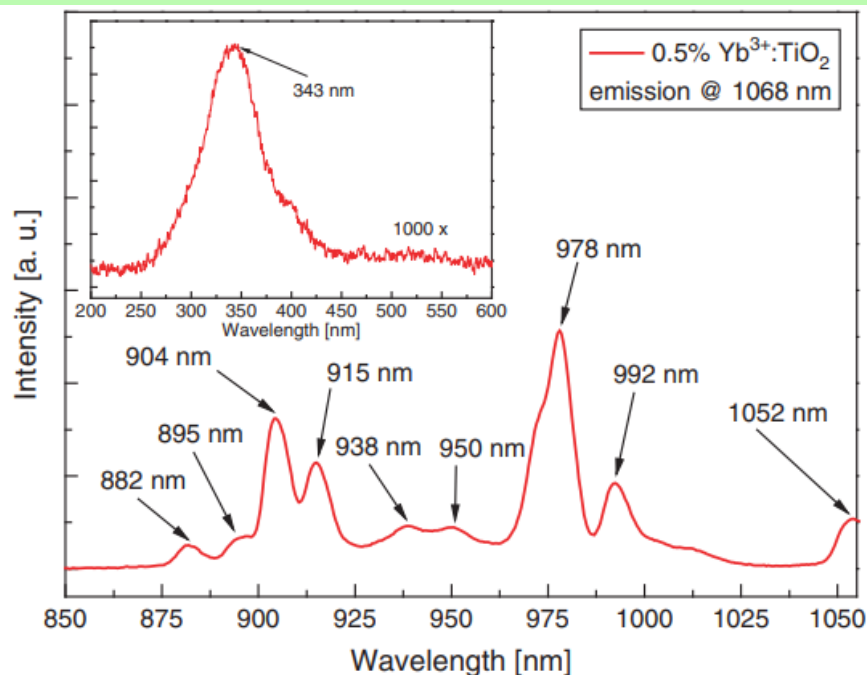


Fig. 5. Excitation spectrum of 0.5 wt.% $\text{Yb}^{3+}:\text{TiO}_2$ nanopowder, monitored at 1068 nm (inset shows the short-wavelength excitation via energy transfer from the TiO_2 matrix).

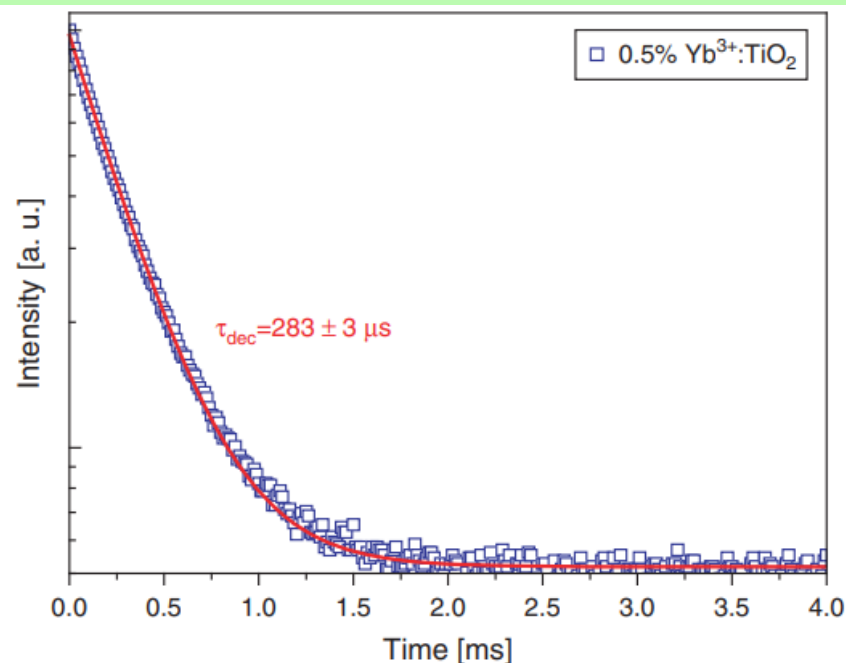


Fig. 7. Decay profile of ${}^2\text{F}_{5/2}$ originating luminescence monitored at 1003,5 nm and recorded for the sample with concentration of 0.5 wt.% of Yb^{3+} .

J. Nanosci. Nanotechnol. 12, 3760–3765, 2012

The $\text{Yb}:\text{TiO}_2$ powders processed with SPVD method exhibits intensive infrared emission with relatively long fluorescence lifetime, which is specifically attractive for further application in up-converting materials co-doped with other RE^{3+} ions dedicated to application in solar converters or photocatalysis.

Optical properties of $\text{TiO}_2\text{:Yb:Nd}$ system (sol-gel method)

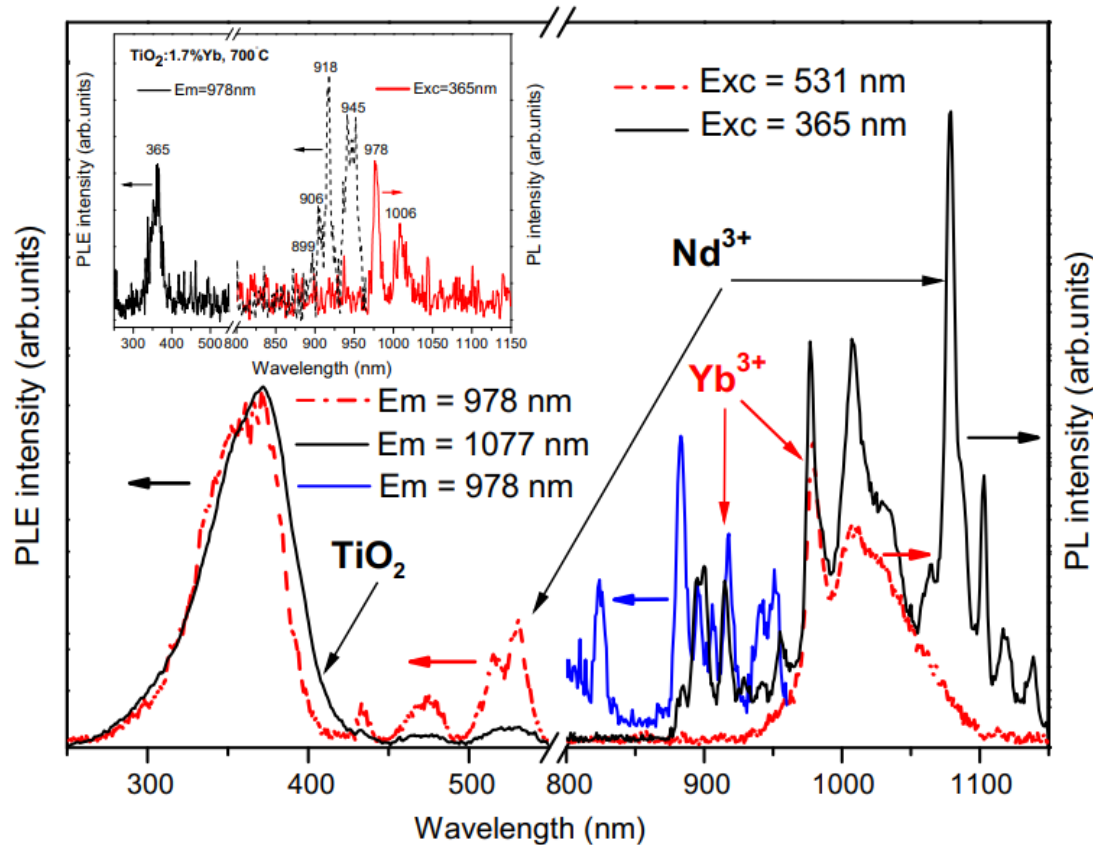


Fig. 4. Luminescence spectra (PLE and PL) of the studied $\text{TiO}_2\text{:Yb(1.7%)}$ and $\text{TiO}_2\text{:Yb(1.7%):Nd(2%)}$ samples. Excitation at $\lambda = 350$ nm (365 nm) and $\lambda = 531$ nm. Inset showing PLE and PL spectra of the $\text{TiO}_2\text{:Yb(1.7%)}$ sample (excitation at $\lambda = 365$ nm).

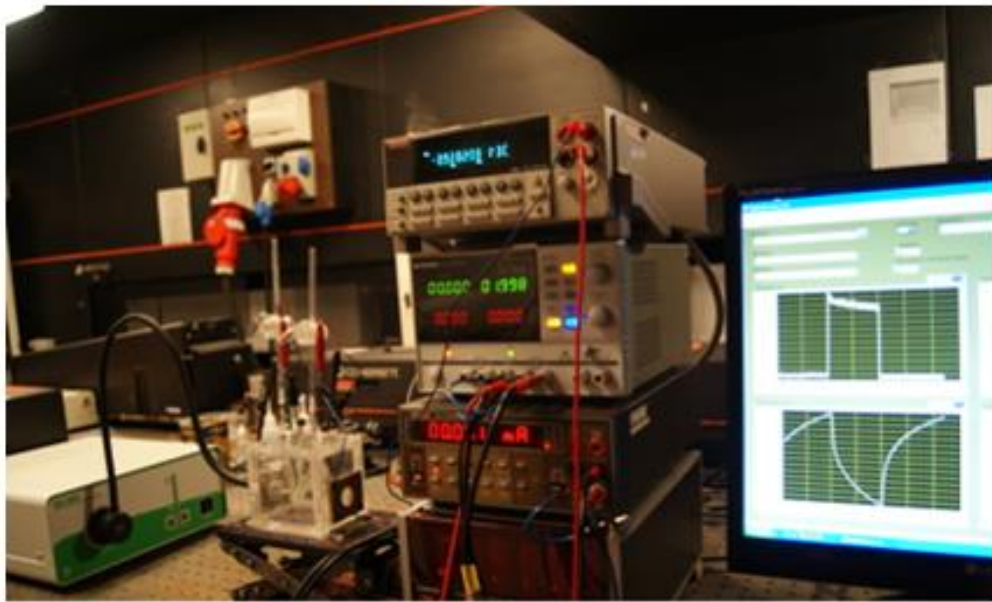
J.D. Fidelus et al. / Optical Materials 47 (2015) 361–365

Due to their strong luminescence, these materials, besides the known photocatalytic activity under solar light, can be taken into account in the silicon solar cells and biological diagnostics applications.

Anode material - obtaining hydrogen by water splitting



TiO₂-ZnO ceramics were obtained by solid solution process in air atmosphere at temperature of 600°C and then the pellets (targets) were sintered at 750°C under solar radiation in nitrogen atmosphere by a Solar Furnace.



1 2 3

Fig. 2. Experimental set up for H₂ generation from water splitting. The individual numbers mean: 1 – the xenon lamp with optical fiber; 2 – the PEC cell; 3 – the monitoring devices.

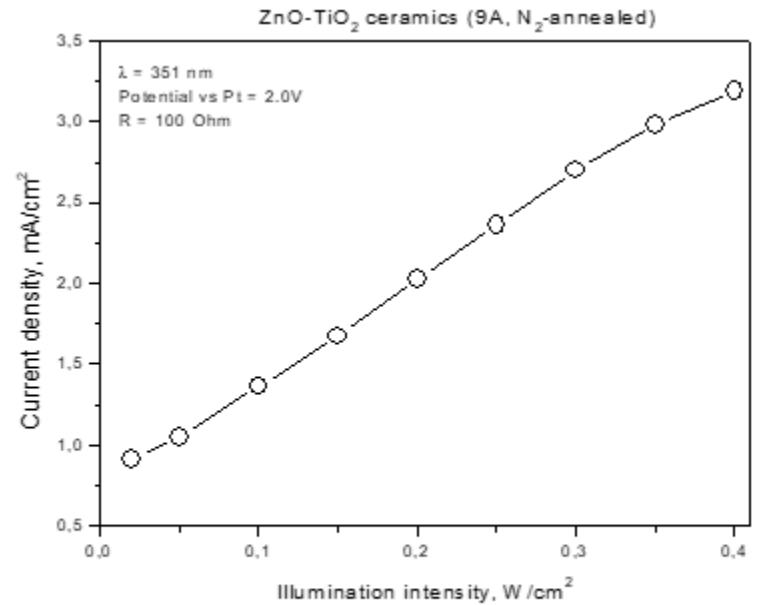
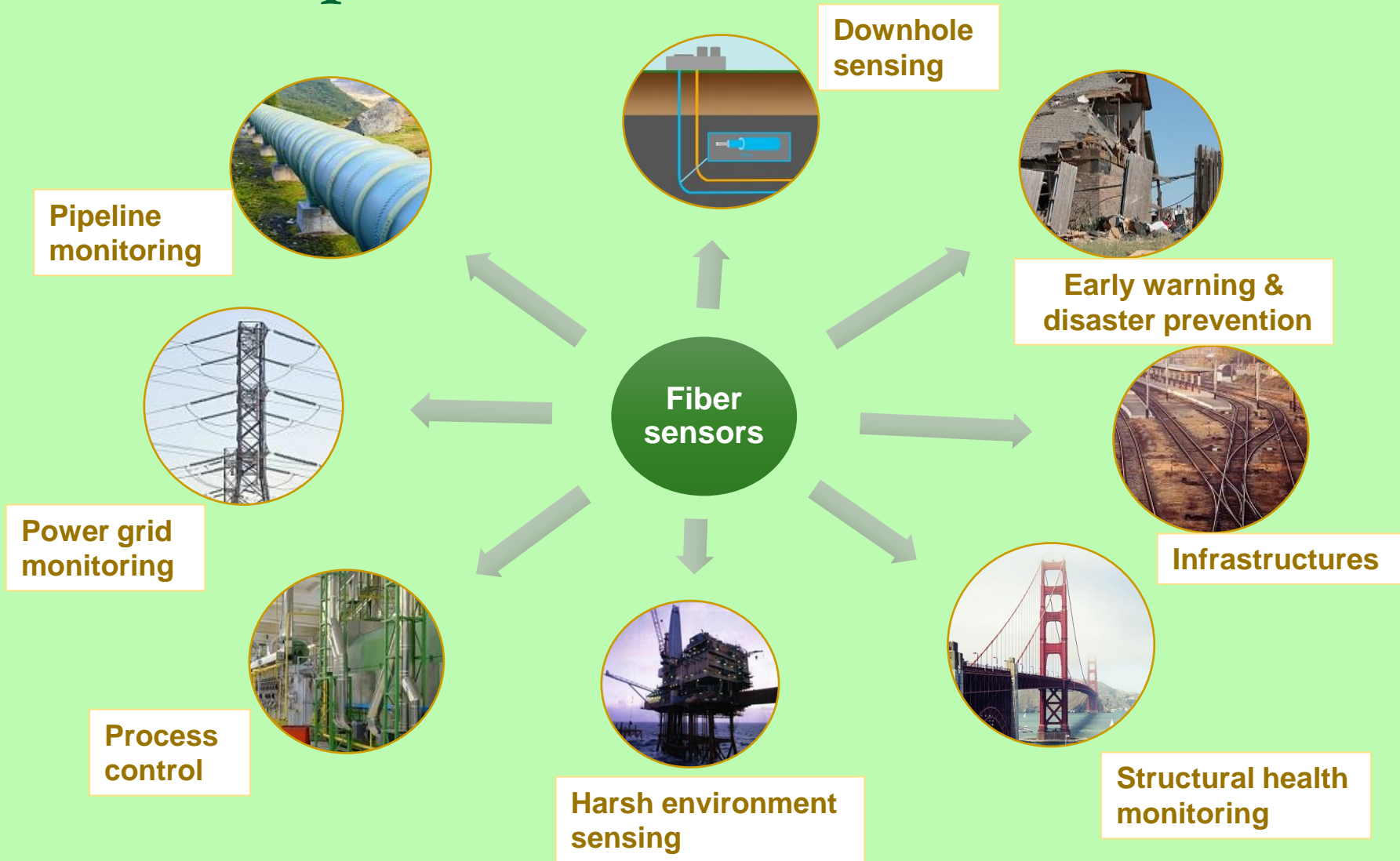


Fig. 5. Photocurrent density of the ZnO-TiO₂ ceramics (9A, N₂) working electrode as a function of illumination intensity.

J.D.Fidelus et al. OMEE-2014

working electrode (ZnO-TiO₂ ceramics), counter-electrode (black platinum), a reference electrode (Ag/AgCl), an electrolyte - sodium sulphate (Na₂SO₄)

Fiber optic sensors



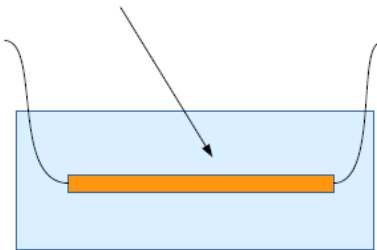
To expand the applications of these materials in difficult conditions and in aggressive alkalis and acids, it is necessary to cover optical fibers with metals

METAL-COATED OPTICAL FIBERS FOR HIGH TEMPERATURE SENSING APPLICATIONS

Metal deposition process

Deposition of metals on selected fragments of optical fibers

Metal coated sensing fragment

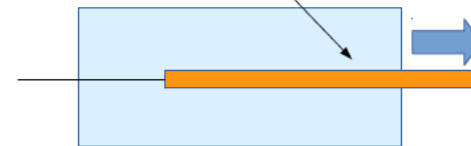


Suitable for:

- FBGs
- LPGs
- FP, MZ and other interferometers
- Microstructures fibers
- Sensor heads
- Other applications

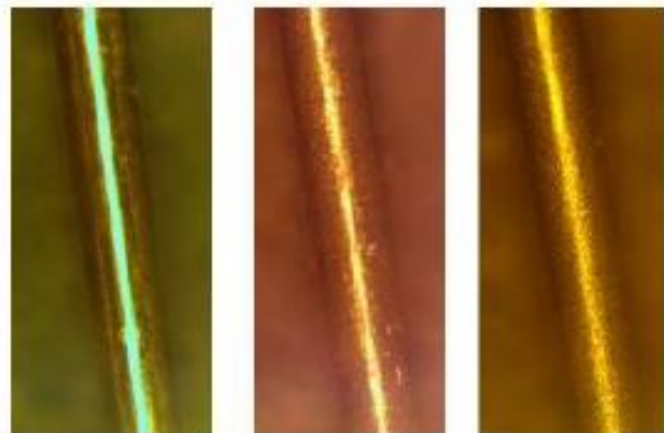
Continuous process of metal deposition on optical fibers

Metal coated optical fiber



Suitable for:

- Data transmission in harsh environments
- Sensor networks at high temperatures
- Distributed sensing of temperature and strain
- Fiber optic Gyroscopes
- Other applications



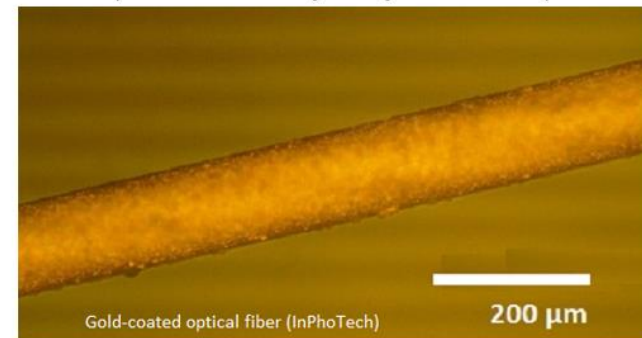
Cu

Ni

Au

GOLD

Metal deposited electrolytically at low temperature.



Gold-coated optical fiber (InPhoTech)

200 μm

Gold coated optical fiber after annealing at 900°C

Possibilities of collaboration between the Physics Department and GUM

Campus in Kielce - basic research and
research and development (R&D) work.

Collaborative projects in the following competitions:

- Polish Metrology
- NCN and NCBiR
- EPM
- Other?

Thank you for your attention

janusz.fidelus@gum.gov.pl